Phenomenological analysis of gluon mass effects in inclusive radiative decays of the J/ψ and Υ

J. H. Field*

Département de Physique Nucléaire et Corpusculaire Université de Genève, 24, Quai Ernest-Ansermet CH-1211 Genève 4, Switzerland

(Received 16 January 2001; published 31 July 2002)

The shapes of the inclusive photon spectra in the processes $J/\psi \to \gamma X$ and $\Upsilon \to \gamma X$ have been analyzed using all available experimental data. Relativistic, higher order QCD, and gluon mass corrections were taken into account in the fitted functions. Only on including the gluon mass corrections were consistent and acceptable fits obtained. Values of $0.721^{+0.016}_{-0.068}$ GeV and $1.18^{+0.09}_{-0.29}$ GeV were found for the effective gluon masses (corresponding to Born level diagrams) for J/ψ and Υ, respectively. The width ratios $\Gamma(V \to \text{hadrons})/\Gamma(V \to \gamma + \text{hadrons})V = J/\psi, \Upsilon$, were used to determine α_s (1.5 GeV) and α_s (4.9 GeV). Values consistent with the current world average α_s were obtained only when gluon mass correction factors, calculated using the fitted values of the effective gluon mass, were applied. A gluon mass $\simeq 1$ GeV, as suggested by these results, is consistent with previous analytical theoretical calculations and independent phenomenological estimates, as well as with a recent, more accurate, lattice calculation of the gluon propagator in the infrared region.

DOI: 10.1103/PhysRevD.66.013013 PACS number(s): 12.38.Qk, 13.25.Gv, 14.70.Dj

I. INTRODUCTION

As suggested by the inventors of QCD [1,2], the color symmetry of the theory is, conventionally, assumed to be unbroken, so that, theoretically [3], the gluon is supposed to have a vanishing mass. It was also conjectured, by the same authors, that the resulting infrared divergences of the theory at large distances (''infrared slavery'') might explain the confinement of quarks. As is also well known, in the contrary case that gluons are massive, there is a possible breakdown of renormalizability as well as violation of unitarity at high energy by certain tree level amplitudes. These problems are common to all non-Abelian gauge theories with massive vector mesons [4,5].

These problems may be solved, as in the standard electroweak model, by the introduction, also for the strong interaction, of spontaneous symmetry breaking and the Higgs mechanism [6]. Since, however, there is no experimental evidence for the existence of a Higgs boson for the strong interaction, or for electrically charged gluons, which are also predicted by some of these ''broken color'' theories, it is still generally supposed, in spite of the infrared divergent nature of such a theory, that the QCD color symmetry remains unbroken.

A possible way out of this dilemma (infrared divergences if the gluon mass is zero, breakdown of renormalizabilty and unitarity if it is not) was indicated by Cornwall [7,8] who suggested that nonvanishing gluon mass might be dynamically generated in a theory in which the color gauge symmetry remained unbroken. Other authors [9,10] pointed out that a gauge invariant, renormalizable, and infrared finite version of QCD with massive gluons is possible, provided that a suitable four-vertex Faddeev-Popov ghost field is introduced into the theory.

The aim of the present paper is not to pursue further these theoretical considerations,[1] but rather to seek *direct experimental evidence* of the mass of the gluon. The processes considered, the radiative decays of ground state vector heavy quarkonia into a photon and light hadrons, are particularly well adapted to such a study, as the observed final state results from the hadronization of a pure two-gluon final state at the lowest order in perturbative QCD (PQCD). These are the ''golden'' physical processes for the determination of the gluon mass, which may be compared to the neutral kaon system for the study of CP violation or tritium β decay for the direct determination of the mass of the electron antineutrino. Indeed, the analogy between the process $J/\psi \to \gamma X$ and tritium β decay is a very close one. In both cases it is the study of the end-point region of a spectrum (that of the electron for tritium β decay, of the photon for the radiative J/ψ decay) that gives the mass limits on the $\overline{\nu_e}$ or the gluon mass. The J/ψ being the lightest quarkonia is the most sensitive to the gluon mass, just as the tritium β decay, with a very low energy release, gives the best direct limit on the $\overline{\nu_e}$ mass. Indeed, as will be shown below, the suppression of the spectrum end point due to gluon mass effects is much more severe in the case of J/ψ radiative decays than for the heavier Υ state.

Already in 1980, Parisi and Petronzio [12] (PP) had suggested a mass of $\simeq 800$ MeV for the gluon, on the basis of the strong suppression of the end point of the photon spectrum in radiative J/ψ decays, as measured by the Mark II Collaboration [13]. However, in order to relate in a precise way the shape of the photon spectrum to the gluon mass, two other important physical effects, which also soften the shape of the photon spectrum, must also be properly accounted for. These are (i) relativistic corrections and (ii) higher order QCD corrections. Because of the only recently available complete next-to-leading-order (NLO) PQCD calculation of the photon spectrum in the decays $\Upsilon \to \gamma X$ [14] and a much improved understanding of the phenomenology of relativistic corrections based on several recent and independent potential model calculations, the analysis presented below is the first to take fully into account the important effects (i) and (ii) and so confirm the conclusion of PP that the gluon mass is $\simeq 1$ GeV. At the time of writing, no calculation yet exists in

*Email address: john.field@cern.ch

[1]The interested reader is referred to Ref. [11] for recent developments, and citations of the related literature.

which the effects (i) and (ii), as well as that of the gluon mass, are taken into account in a unified way, so the present analysis is inevitably a phenomenological one where the three different types of corrections are assumed, loosely speaking, to ''factorize.'' Since, however, it is clear that the gluon mass effects are by far the most important, no large uncertainty on the results obtained is expected to result from this approximation.

The results presented below also confirm the conclusions of two previous, closely related, papers written by Consoli and the present author [15,16] (CF1,CF2). Some brief comments are made here on these papers: some more detailed remarks are made in Sec. VIII below.

In CF1 effective gluon masses m_g determined from fits to $J/\psi \to \gamma X$ and $\Upsilon \to \gamma X$ were used, in conjunction with gluon mass correction factors calculated by PP (or recalculated using pure phase-space considerations) to derive a large number of α_s values from different charmonium and bottomonium branching ratios. Agreement with the expected PQCD evolution of α_s from the scale $M_{J/\psi}/2$ to $M_\Upsilon/2$ was only obtained when the gluon mass corrections were applied. Also only in this case was good agreement found between the derived values of α_s and those obtained from deep inlastic scattering experiments. In this paper only the Photiadis [17] higher order (HO) QCD correction (which is only applicable in the end-point region of the photon spectrum, and does not include real gluon radiation effects) was used, and relativistic corrections were completely neglected.

The second paper, CF2, made essential use of the recently proposed nonrelativistic quantum chromodynamics (NRQCD) formalism of Bodwin, Braaten, and Lepage (BBL) [18], in which both nonrelativistic and HO QCD corrections (but not gluon mass effects) were treated in a rigorous way, order by order in perturbation theory, using an operator product expansion. As suggested by BBL, the values of α_s and the leading relativistic correction parameter $r \simeq \langle v^2 \rangle$ were treated as free parameters in fits to various charmonium and bottomonium decay widths. Similar fits were also performed to the inclusive photon spectra in J/ψ and Υ decays. No consistent values of r and α_s were found in the absence of gluon mass corrections. When the latter were included, consistent values of α_s similar to those found in CF1 were obtained. However, in this case, the values of r were found to be much smaller in absolute value than the expectations from potential model calculations, and even (as discussed further in Sec. VIII below) of the wrong sign. The conclusion concerning the inability of the NRQCD formalism to describe the experimental data, in the absence of gluon mass corrections, was not, however, affected by the incorrect treatment of relativistic corrections.

The structure of this paper is as follows. Sections II, III, and IV are devoted to descriptions of the implementation of relativistic, HO QCD, and gluon mass corrections, respectively. Fits to the experimental data on $J/\psi \to \gamma X$ and $\Upsilon \to \gamma X$ to obtain, in each case, the corresponding effective gluon mass m_g, are described in Secs. V and VI. Section VII describes the determination of $\alpha_s(m_c)$ and $\alpha_s(m_b)$ from the experimental branching ratios $\Gamma(V \to \text{hadrons})/\Gamma(V \to \gamma + \text{hadrons})$, $V = J/\psi, \Upsilon$. The values of α_s obtained in this way are unaffected by relativistic corrections. In Sec. VIII, the effective gluon mass values obtained in this paper are compared with other estimates of the gluon mass in the literature. Finally, Sec. IX contains a brief summary and outlook. Details of the method used to simulate the effects of experimental resolution on the inclusive photon spectrum are given in an Appendix.

II. RELATIVISTIC CORRECTIONS

Relativistic corrections to the van Royen–Weisskopf formula [19] for the decay rate of a vector meson V into a charged lepton pair,

$$\Gamma(V \to l^+ l^-) = \frac{16\pi\alpha(M_V)^2 e_Q^2}{M_V^2} |\psi(0)|^2, \tag{2.1}$$

were calculated by Bergström *et al.* [20]. A relativistic correction factor f_{RC} to the leptonic decay width $\Gamma(V \to l^+ l^-)$ was found with the general form

$$f_{RC}(V \to l^+ l^-) = \left(1 - \frac{1}{3} r\right)^2 \tag{2.2}$$

where

$$r = \int \frac{d^3p}{(2\pi)^3} \frac{[E(p) - m_Q]}{E(p)} \frac{\tilde{\psi}(p)}{\psi(0)} \tag{2.3}$$

and E, p, and m_Q are the energy, momentum, and mass of the bound heavy quark. $\tilde{\psi}(p)$ is the wave function in relative momentum space, related to the spatial wave function at the origin, $\psi(0)$, by the expression

$$\psi(0) = \int \frac{d^3p}{(2\pi)^3} \tilde{\psi}(p). \tag{2.4}$$

In the approximation where the valence quarks of the vector meson are considered to be symmetrically bound in the meson rest frame, so that $E(p) = M_V/2$, it follows that

$$\begin{aligned} \frac{E(p) - m_Q}{E(p)} = \frac{\epsilon}{M_V} &= \frac{\sqrt{p^2 + m_Q^2} - m_Q}{M_V/2} \\ &= \frac{p^2}{m_Q M_V} + O(p^4) \\ &= \frac{p^2}{2m_Q^2} + O(p^4) \\ &= \frac{v^2}{2} + O(v^4). \end{aligned} \tag{2.5}$$

Here ϵ is the "binding energy" $M_V - 2m_Q$ and v is the velocity of the heavy quark.[2] Using Eq. (2.5), Eq. (2.2) may be written as

$$f_{RC}(V\to l^+l^-)=\left(1-\frac{1}{6}\langle v^2\rangle\right)^2+O(v^6) \tag{2.6}$$

where $\langle v^2\rangle$ is the mean value of the squared velocity, which depends on the bound state potential. Similar relativistic corrections were calculated for several decay processes of heavy quarkonia by Keung and Muzinich (KM) [21]. The calculation was based on a nonrelativistic reduction of the Bethe-Salpeter equation [22] for the relativistic quark-antiquark bound state problem. The results of KM were presented as $O(v^2)$ corrections to the decay rate rather than to the decay amplitude, as in Eq. (2.6) above. In the present paper all relativistic corrections are applied at the amplitude level so that additional $O(v^4)$ terms are added to the results quoted by KM to "complete the square" and obtain a positive definite decay rate. This correction is important only for charmonium decays where, because of the relatively large value of $\langle v^2\rangle$, the corrected decay rate becomes negative for both small and large values of $z\equiv 2E_\gamma/M_V$, if only the $O(v^2)$ correction terms are retained. KM confirm the relativistic correction factor for $V\to l^+l^-$ given in Eq. (2.6) and find also

$$f_{RC}(V\to ggg)=f_{RC}(V\to \gamma gg)=(1-2.16\langle v^2\rangle)^2+O(v^6). \tag{2.7}$$

Of particular importance for the present study, KM also give, in their Eq. (3.5), the relativistic correction to the inclusive photon spectrum in $V\to\gamma gg$. "Completing the square" to obtain a positive definite differential decay rate yields the spectrum

$$\frac{1}{\Gamma}\frac{d\Gamma}{dz}=\frac{1}{C_N}\left[\sqrt{f_0(z)}+\frac{g(z)\langle v^2\rangle}{2\sqrt{f_0(z)}}\right]^2 =\frac{1}{C_N}\left[f_0(z)+g(z)\langle v^2\rangle+\frac{[g(z)\langle v^2\rangle]^2}{4f_0(z)}\right], \tag{2.8}$$

where [23]

$$C_N=(\pi^2-9)\left[1+\langle v^2\rangle\left(\frac{5}{3}-\frac{1}{4}\frac{(9\pi^2-68)}{(\pi^2-9)}\right)\right] \sim(\pi^2-9)(1-4.32\langle v^2\rangle) \tag{2.9}$$

and

$$g(z)\equiv\frac{5f_0(z)}{3}-\frac{f_1(z)}{12}. \tag{2.10}$$

The functions $f_0(z)$ and $f_1(z)$ are reported in Eqs. (15) and (16) of Ref. [16]. In the approximation used here, relativistic corrections are completely specified by the single parameter $\langle v^2\rangle$. Although one may hope, in the future, to determine this nonperturbative parameter by lattice QCD methods [24], the only existing estimates are derived from potential models of the quarkonium bound state. Some of the estimates of $\langle v^2\rangle$ for the J/ψ and the Υ that have been given in the literature are presented in Table I. Usually in these papers the relativistic correction factor for the decay $V\to l^+l^-$ is quoted. For the entries in Table I, this is converted into a value of $\langle v^2\rangle$ using Eq. (2.6). In the case of Chiang *et al.* [25] Eq. (2.7) is used, and for Chao *et al.* [26] the ratio $f_{RC}(V\to ggg)/f_{RC}(V\to l^+l^-)$. Schuler [27] directly calculated values of $\langle v^2\rangle$ for a series of different charmonium and bottomonium states as a function of the parameter ν in a power-law potential of the form $V(r)=\lambda r^\nu$. The range of different values of $\langle v^2\rangle$ presented in Table I is very wide: 0.20–0.47 for the J/ψ and 0.048–0.47 for the Υ. Apart from the estimates of Bergström *et al.* [32] and Beyer *et al.* [28] the value of $\langle v^2\rangle$ is found to be significantly larger for the J/ψ than for the Υ, as intuitively expected, given the smaller mass of the charm quark. The near equality of the values of $\langle v^2\rangle$ for the J/ψ and the Υ and the very large value found for the Υ in Refs. [32] and [28] may be a consequence of an extreme choice of the parameters of the potential in the case of the Υ.

TABLE I. Estimations of $\langle v^2\rangle$ for the J/ψ and the Υ.

Reference	J/ψ	Υ
Bradley [29]	0.44	0.069
Eichten *et al.* [30]	0.20	0.096
Bergström *et al.* I [31]		
$V(r)=0.2r-0.25/r$	0.47	—
$V(r)=\frac{1}{2}\mu\omega_0^2r^2$	0.21	—
$V(r)=\mathrm{Tr}-\alpha_s(r)/r$	0.34	—
Bergström *et al.* II [32]		
$V(r)=0.2r-4\alpha_s/3r$	0.47	—
$V(r)=0.163r-4\alpha_s/3r$	—	0.47
Beyer *et al.* [28]	0.21	0.18
Chiang *et al.* [25]	0.21	0.078
Chao *et al.* [26]	0.26	0.13
Schuler [27]		
$V(r)=\lambda r^\nu$		
$\nu=-0.1$	0.36	0.075
$\nu=0.0$	0.32	0.066
$\nu=0.3$	0.25	0.048

In the present paper, more weight is given to the more recent results of Chiang *et al.*, Chao *et al.*, and Schuler, which are roughly consistent with each other. In the following, the values taken are $\langle v^2\rangle=0.28$ for the J/ψ and $\langle v^2\rangle=0.09$ for the Υ, which lie near the middle of the range of values obtained by these last three authors. As it will be seen that the effects of relativistic corrections on the shape of the fitted photon spectra are, after the inclusion of gluon mass effects, small (as already conjectured in Refs. [15,16]), the conclusions of the present work are not sensitive to the pre-

[2]In units with $c=1$.

cise values assumed for $\langle v^2 \rangle$. The relativistically corrected inclusive photon spectra for the J/ψ and the Υ calculated using Eq. (2.8) are shown, in comparison with the lowest order (LO) QCD prediction [33], in Figs. 1(a) and 1(b), respectively. Also shown in Fig. 1(a) is the curve given by truncating the correction to the decay rate above $O(v^2)$. In this case the spectrum is set to zero if the prediction is negative. It may be remarked that Eq. (2.8) shows singular behavior as $z \to 0$.[3] However, this does not affect any of the fits presented below, as no experimental measurements exist for $z < 0.2$.

III. HIGHER ORDER QCD CORRECTIONS

To lowest order in perturbative QCD, the inclusive photon spectrum is described by the process $V \to \gamma gg$. Assuming massless gluons and neglecting relativistic corrections, the shape of the photon spectrum is the same as in orthopositronium decay [33]:

$$\frac{1}{\Gamma}\frac{d\Gamma}{dz} = \frac{1}{(\pi^2-9)}\left[\frac{4(1-z)\ln(1-z)}{z^2} - \frac{4(1-z)^2\ln(1-z)}{(2-z)^2} + \frac{2z(2-z)}{z^2} + \frac{2z(1-z)}{(2-z)^2}\right]. \tag{3.1}$$

The first estimation of higher order QCD corrections to the spectrum was made by Field [34]. These QCD effects were calculated using a parton shower Monte Carlo program in which the process $g \to gg$ was iterated. The invariant mass of the cascading virtual gluons was cut off at the scale $\mu_c = 0.45$ GeV and a value $\Lambda = 0.2$ GeV was used for the QCD scale parameter in the parton shower. For Υ decays the average, perturbatively generated, ''effective gluon mass,'' i.e., the mass of the virtual gluon initiating the parton cascade, was 1.6 GeV. Because of the low value of the cutoff scale, the shapes of the photon spectra for J/ψ and Υ decays were predicted to be similar. In both cases the average value of z was found to be 0.57, and even in the case of the decay of a hypothetical state with a mass of 60 GeV, the average z increased only to 0.59. The Field [34] spectrum for Υ decays is shown in Fig. 2 as the dotted line. The parton cascade used in [34] does not take into account QCD coherence effects in gluon radiation [35] usually implemented in parton shower Monte Carlo event generators by an ''angular ordering'' ansatz [36]. The effect of this coherence, which is the QCD analogue of the ''Chudakov effect'' [37] in QED, is to suppress corrections due to real gluon radiation for kinematical configurations that yield photons close to the kinematical end point. In this case the two primary recoiling gluons are almost collinear, forming an effectively colorless current from which the radiation of large angle secondary gluons is strongly suppressed by destructive interference [38]. The radiation of almost collinear gluons is not suppressed, but such radiation will hardly modify the shape of the LO spectrum. It is thus to be expected that the neglect of QCD coherence in the parton shower used to calculate the Field spectrum will result in a too strong suppression of the spectrum in the end-point region. The comparison, shown below, with a complete NLO perturbative QCD calculation, where such coherence effects are taken into account, indicates that this is indeed the case. The Field spectrum gives a good description of four out of five of the experimental measurements of the Υ spectrum (see Sec. VI below). It will be seen, however, that, for the case of J/ψ decays, the spectrum is much too hard to describe the experimental measurements.

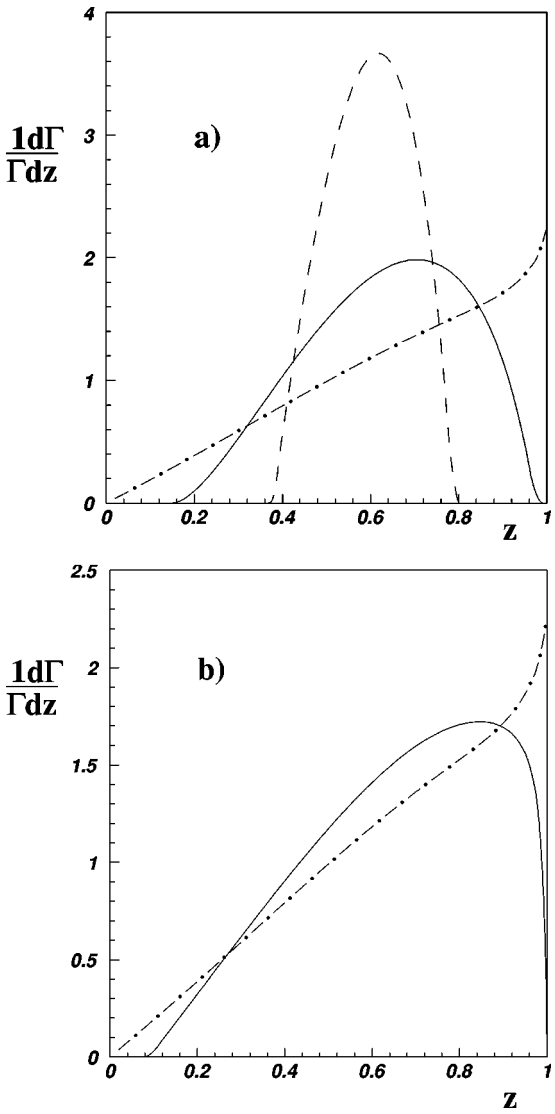

FIG. 1. Theoretical predictions for relativistic corrections to the inclusive photon spectrum in (a) J/ψ, and (b) Υ, radiative decays. In (a), the LO QCD prediction [33] is shown as the dot-dashed line. The solid line gives the prediction of Eq. (2.8) for $\langle v^2 \rangle = 0.28$. The dashed line shows the prediction of Eq. (2.8) neglecting the order $\langle v^2 \rangle^2$ term. In this case only the positive part of the prediction is shown. In (b), the LO QCD prediction [33] is again shown as the dot-dashed line. The solid line gives the prediction of Eq. (2.8) for $\langle v^2 \rangle = 0.09$. In both (a) and (b) the peak of the function in Eq. (2.8) at small values of z has been suppressed.

The second estimate of higher order QCD corrections to

[3]The corresponding peaks near $z = 0.0$ are suppressed in Fig. 1.

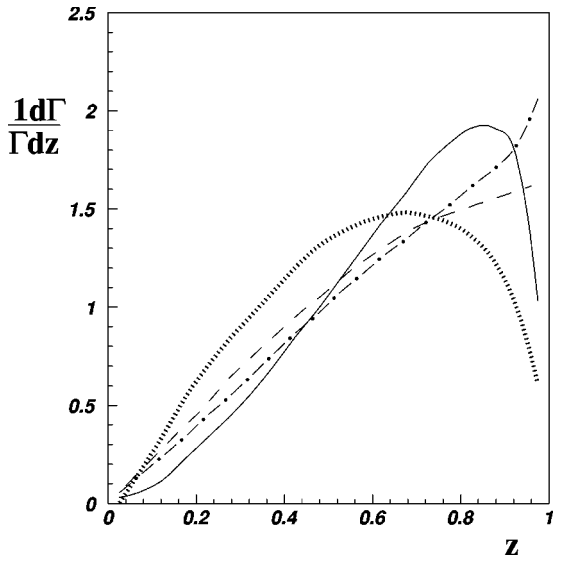

FIG. 2. QCD predictions for the inclusive photon spectrum in radiative Υ decays. Dot-dashed, LO [33]; dotted, Field [34]; dashed, Photiadis [17]; solid curve, Krämer (NLO) [14].

the inclusive photon spectrum in Υ decays was made by Photiadis [17]. This calculation, expected to be valid near $z=1$, completely neglected real gluon radiation, which, as discussed above, is strongly suppressed in this region, but resummed to all orders in α_s the leading logarithmic terms of the form $\ln(1-z)$ resulting from the exchange of virtual gluons and quarks between the two recoiling gluons of the LO diagram. As shown in Fig. 2 (the dashed curve), these effects give only a modest suppression of the LO spectrum near $z=1$.

The most recent result on higher order QCD corrections to the Υ spectrum is the complete NLO calculation of Krämer [14] that is also shown in Fig. 2 as the solid curve. It can be seen that strong suppression occurs only very near to $z=1$, and is much less marked than in the case of the Field spectrum.

Since the Photiadis calculation does not include the effects of real gluon radiation, it can be argued that the corrections calculated by both Krämer and Photiadis should be applied. This will double count virtual corrections of the type shown in Fig. 2(c) of Ref. [14], but should give a better description, particularly away from the end-point region, than using only the Photiadis correction.

To date, no calculations of the inclusive photon spectrum in heavy quarkonia decays have been made that take into account, at the same time, higher order QCD corrections, relativistic corrections, and genuine gluon mass effects.[4] Indeed, since the pioneering paper of PP [12], gluon mass effects have been completely calculated only for the LO processes $V\to ggg$ and $V\to\gamma gg$ [39] (see Sec. IV below).

In the present analysis, the higher order QCD calculations of Photiadis and Krämer, made for Υ decays, are also used, unmodified, for J/ψ decays. In fact it will be seen that the observed end-point suppression of the photon spectrum of the J/ψ is so large, as compared to the predicted effect of both relativistic and higher order QCD corrections, that these play only a minor role. Indeed, the value of the effective gluon mass m_g needed to describe the experimental spectrum is little affected by the inclusion of these corrections. The ansatz used to apply the higher order QCD corrections is to multiply the relativistically corrected photon spectrum given by Eq. (2.8) by the QCD correction factor

$$C_{QCD}=\frac{d\Gamma_{HO}}{dz}/\frac{d\Gamma_{LO}}{dz}. \tag{3.2}$$

In the case of fits with $m_g\neq 0$, phase-space limitations are taken into account by the replacement $z\to z/z_{MAX}$ in Eq. (3.2) where

$$z_{MAX}=1-\frac{4m_g^2}{M_V^2}. \tag{3.3}$$

In view of the large value found for the ratio m_g/M_V for the J/ψ, it is to be expected that phase-space suppression effects will be even more important for the HO corrections than for the LO process. This will reduce even further the effect of such corrections on the fitted value of m_g.

IV. GLUON MASS EFFECTS

The possibility of gluon mass effects in the decay $J/\psi\to\gamma X$ was first considered by PP [12]. They noted that the very strong suppression of the end-point region of the photon spectrum measured by the Mark II Collaboration [13] could be explained by introducing a gluon mass of about 0.8 GeV. The comparison of the PP prediction with the experimental data did not, however, take into account experimental resolution effects, which are very large in this case. Also, relativistic and higher order QCD corrections were not included. The aim of the present paper is perform a similar comparison to that made by PP, but using all available experimental data on both J/ψ and Υ radiative decays, as well as including experimental resolution effects, relativistic corrections, and higher order QCD corrections. As the last two effects also suppress the end-point region of the photon spectrum, only a complete quantitative analysis, including all relevant effects, can show if the introduction of a nonvanishing effective gluon mass is required to describe the experimental data.

Introducing an ''effective gluon mass'' in the calculation of the Born diagram has two effects: (i) restriction of the

[4]That is, including a fixed gluon mass in the calculation of both the invariant amplitude and the phase space, and taking into account the longitudinal polarization states of the gluons. This is to be contrasted with the parton shower model of Field where an effective gluon mass (actually a timelike gluon virtuality) is perturbatively generated from massless gluons. The distinction between ''genuine'' and ''effective'' gluon masses is discussed further in Sec. IV.

TABLE II. Photon energy resolutions of the different heavy quarkonia radiative decay experiments.

Experiment	Decay process	$f_{E_\gamma}=\sigma_{E_\gamma}/E_\gamma$(GeV)	f_{E_γ} at $E_\gamma=M_V/2$ (%)
Mark II	$J/\psi\to\gamma X$	$0.12/\sqrt{E_\gamma}$	9.6
	$\psi'\to\pi^+\pi^-(J/\psi\to\gamma X)$	$0.12/\sqrt{E_\gamma}$	9.6
	$J/\psi\to(\gamma\to e^+e^-)X$	$0.022E_\gamma^{0.25}$	3.4
CUSB	$\Upsilon\to\gamma X$	$0.039/E_\gamma^{0.25}$	3.2
ARGUS	$\Upsilon\to\gamma X$	$\sqrt{0.0052+0.0042/E_\gamma}$	7.8
Crystal Ball	$\Upsilon\to\gamma X$	$0.027/E_\gamma^{0.25}$	1.8
CLEO2	$\Upsilon\to\gamma X$	$0.0035/E_\gamma^{0.75}+0.019-0.001E_\gamma$	1.5

available phase space, i.e., modification of the boundary of the Dalitz plot; (ii) contributions to the amplitude from longitudinal gluon polarization states. As will be seen, effect (i) is by far the most important.

The gluon mass is ''effective'' because it is defined only at the level of the Born diagram. When such a prediction is fitted to the data, which include QCD corrections to all orders, the value of m_g is expected to be different from the value obtained if the gluon mass were correctly included also in higher order diagrams in the prediction. In fact, a ''genuine'' gluon mass M_g might be operationally defined as the effective mass corresponding to a hypothetical all-orders PQCD calculation with massive gluons. If phase-space limitations are very important, as in the case of the J/ψ, the tree level ''effective'' value is expected to be lower than the ''genuine'' value that would be found in a fit that properly included gluon mass effects at all orders. If, on the other hand, the ''genuine'' gluon mass is small compared to that of the decaying state, the effects of the nonvanishing gluon mass will be limited to a small region near the boundaries of phase space. In this case the tree level ''effective'' mass is mainly generated perturbatively by splitting into gluon and quark pairs (as in the Field model) and is expected to be much larger than the ''genuine'' value. However, the ''genuine'' mass M_g found by comparing the prediction of the all-orders PQCD calculation to the data is expected to be independent of the mass of the decaying state. The above argument also shows that, for some mass of the decaying state, the tree level ''effective'' mass and the ''genuine'' gluon mass should be equal. It may be conjectured that this is almost the case for the Υ.

The correction curves for the processes $J/\psi\to ggg$ and $\eta_c\to gg$ calculated by PP and shown in their Fig. 1 took into account both the effects (i) and (ii), but no explicit formulas were given. In the present paper essential use is made of formulas including both effects (i) and (ii) obtained by Liu and Wetzel [39]. For the decay $V\to\gamma gg$, the fully differential spectrum is

$$\frac{1}{\Gamma_0}\frac{d\Gamma}{dzdx_1dx_2}=\frac{1}{(\pi^2-9)}\frac{1}{z^2(x_2')^2(x_3')^2}\left[\frac{8}{3}\eta\left(1-\frac{25}{2}\eta\right)(1-2\eta)^2+32z(1-2\eta)\left(1-\frac{\eta}{4}\right)\eta^2+z^2(1-2\eta)(1-6\eta-6\eta^2)\right.$$
$$-2[z^3+(x_2')^3+(x_3')^3]\left(1-\frac{10}{3}\eta-2\eta^2\right)+z^4\left(1+\frac{\eta}{2}\right)+[(x_2')^2+(x_3')^2](1-8\eta+22\eta^2+8\eta^3)$$
$$\left.-(x_2')^2(x_3')^2\eta+[z^4+(x_2')^4+(x_3')^4]\left(1+\frac{\eta}{2}\right)\right], \tag{4.1}$$

where $z\equiv 2E_\gamma/M_V$, $\eta\equiv(m_g/M_V)^2$, $x_i\equiv 2E_i/M_V$, $x_i'\equiv x_i-2\eta$, and $E_i=$gluon energy. Here Γ_0 is the radiative width uncorrected for gluon mass effects. The allowed phase space region is defined by the conditions[5]

$$2=z+x_2+x_3, \tag{4.2}$$

$$0\leqslant z\leqslant 1-4\eta, \tag{4.3}$$

$$x_2^{min}\leqslant x_2\leqslant x_2^{max}, \tag{4.4}$$

$$x_2^{max}=1-\frac{z}{2}\left[1-\sqrt{1-\frac{4\eta}{1-z}}\right], \tag{4.5}$$

$$x_2^{min}=1-\frac{z}{2}\left[1+\sqrt{1-\frac{4\eta}{1-z}}\right]. \tag{4.6}$$

In the gluon mass dependent fits to be presented below, the functions $f_0(z)$ and $f_1(z)$ in the KM formula (2.8) are replaced by the functions

[5]Note that η is defined differently here from in Ref. [16].

$$f_0(z,m_g)=\int_{x_2^{min}}^{x_2^{max}} dx_2 f_0(z,x_2,m_g), \tag{4.7}$$

$$f_1(z,m_g)=\int_{x_2^{min}}^{x_2^{max}} dx_2 f_1(z,x_2), \tag{4.8}$$

where $f_0(z,x_2,m_g)$ is derived from Eq. (4.1) of this paper and $f_1(z,x_2)$ from Eq. (3.5) of KM. Thus phase-space effects are taken properly into account in both f_0 and f_1, whereas the effects of longitudinal polarization states are included only in f_0. As will be shown below, the latter effect is much smaller than the former, so that the effect on the fit results of the uncalculated contribution of gluon longitudinal polarization states on the relativistic correction coefficient f_1 is expected to be completely negligible.

V. THE DECAY $J/\psi\rightarrow\gamma X$

To date, the inclusive photon spectrum in J/ψ decays has been measured by only one experiment, the Mark II Collaboration [13]. Actually, in Ref. [13], three independent measurements of the spectrum are given. The first (referred to simply as ''Mark II'') uses the process

$$e^+e^-\rightarrow J/\psi\rightarrow\gamma X$$

where the photons are detected in the electromagnetic calorimeter of the detector. The second sample, ''Mark II(cascade),'' uses the process

$$e^+e^-\rightarrow\psi'\rightarrow J/\psi\pi\pi\rightarrow\gamma X\pi\pi.$$

In this case the acceptance and resolution are similar to those in the Mark II measurement. The third data sample, ''Mark II(conversion),'' uses J/ψ radiative decay events where the photon converts into an e^+e^- pair in the beam pipe or the inner flange of the tracking chamber. Measurement of the momenta of the e^+,e^- in the chamber yields a sample with reduced statistics but much improved photon energy resolution The photon energy resolutions for these three event samples are given in Table II.

As well as these inclusive measurements, many exclusive measurements have been made where a single resonant state or an exclusive multihadron final state is produced in association with a hard photon [3]. These measurements are summarized in Table III where the values of z for each exclusive channel with a single particle recoiling against the photon are given. As can be seen from Table III (see also Fig. 59 of Ref. [40]) the most striking feature of the photon spectrum near the end point is the strong exclusive production of η and η' mesons:

$$J/\psi\rightarrow\gamma\eta,\gamma\eta'.$$

These two channels alone account for 13% of the total branching ratio (BR) for $z>0.6$ and completely dominate the end-point region $z>0.85$. Because of the large contribution of these two resonances, it was not possible to obtain acceptable fits to the J/ψ spectra using the function of Eq. (2.8)

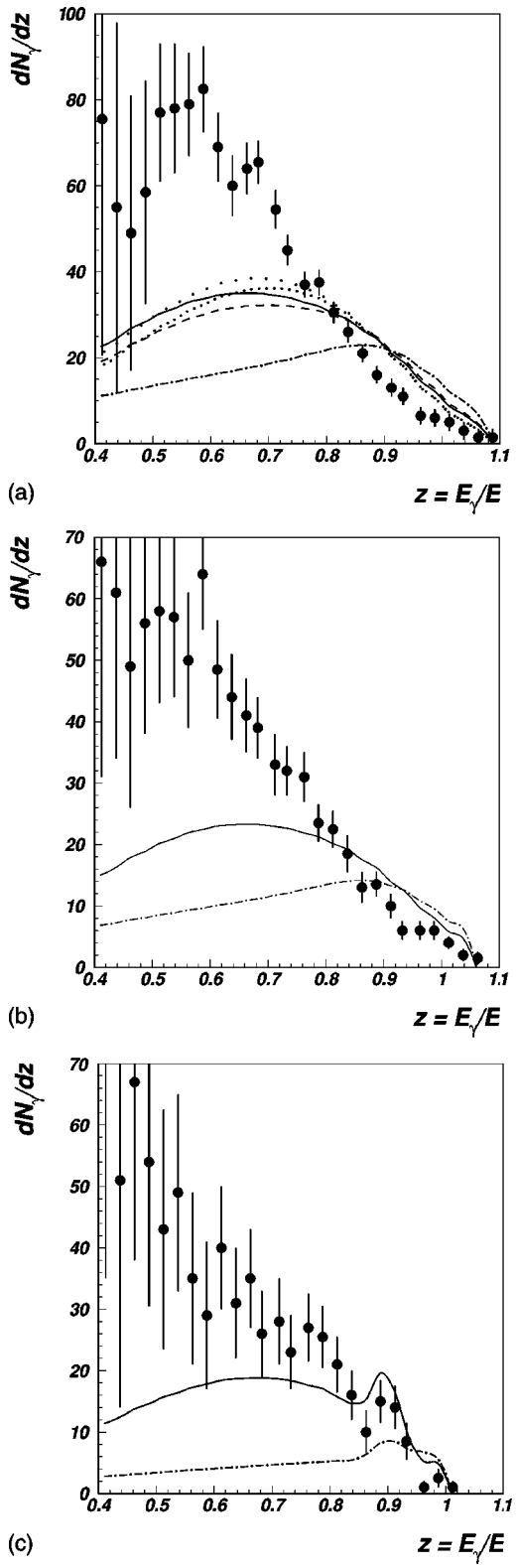

FIG. 3. Fits, assuming $m_g=0$, to inclusive photon spectra in J/ψ decays. Mark II (top left), Mark II cascade (top right), Mark II conversion (bottom). Dash-dotted line, LO QCD prediction [33]; dashed line, relativistic correction (RC) included [21]; solid line, RC and Photiadis [17] HO QCD correction; fine dotted line, RC and Krämer [14] HO QCD correction; and dotted line, RC, Photiadis, and Krämer corrections.

TABLE III. Composition of the hadronic final state in the $J/\psi \to \gamma C$ radiative decays: $J/\psi \to \gamma C$ [3].

Channel C	z	BR$\times 10^4$	Relative BR
	Resonances		
π^0	0.998	0.39 ± 0.13	0.009
η	0.969	8.6 ± 0.8	0.2
η'	0.904	43.1 ± 3.0	1.0
$\eta(1440) \to \rho\rho$	0.784	17.0 ± 4.0	0.39
$\eta(1440) \to \rho\gamma$	0.784	0.64 ± 0.14	0.015
$\eta(1440) \to K\bar{K}\pi$	0.784	9.1 ± 1.8	0.21
$\eta(1440) \to \eta\pi^+\pi^-$	0.784	3.0 ± 0.5	0.07
$\eta(1760) \to \rho\rho$	0.677	1.3 ± 0.9	0.030
$\eta_2(1870) \to \pi\pi$	0.63	6.2 ± 2.4	0.144
$\eta(2225)$	0.484	2.9 ± 0.6	0.067
$f_2(1270)$	0.832	13.8 ± 1.4	0.32
$f_1(1285)$	0.828	6.1 ± 0.9	0.14
$f_1(1420) \to K\bar{K}\pi$	0.790	8.3 ± 1.5	0.19
$f_0(1500)$	0.765	5.7 ± 0.8	0.13
$f_1(1510) \to \eta\pi^+\pi^-$	0.762	4.5 ± 1.2	0.10
$f_2'(1525)$	0.758	4.7 ± 0.6	0.11
$f_0(1710) \to K\bar{K}$	0.695	8.5 ± 1.0	0.20
$f_2(1950) \to K^*\bar{K}^*$	0.603	7.0 ± 2.2	0.16
$f_4(2050)$	0.561	27.0 ± 7.0	0.63
$f_J(2220) \to \pi\pi$	0.486	0.8 ± 0.4	0.019
$f_J(2220) \to K\bar{K}$	0.486	0.8 ± 0.3	0.019
$f_J(2220) \to p\bar{p}$	0.486	0.15 ± 0.08	0.003
Total BR (Resonance)		180 ± 10	4.17
	Exclusive states		
$\pi^+\pi^-\pi^0\pi^0$	–	83.0 ± 31.0	1.93
$\pi^+\pi^-\pi^+\pi^-$	–	28.0 ± 5.0	0.65
$K^+K^-\pi^+\pi^-$	–	21.0 ± 6.0	0.49
$\eta\pi\pi$	–	61.0 ± 10.0	1.42
$\rho\rho$	–	45.0 ± 8.0	1.05
$\omega\omega$	–	15.9 ± 3.3	0.37
$\phi\phi$	–	4.0 ± 1.2	0.093
$K^*\bar{K}^*$	–	40.0 ± 13.0	0.92
$p\bar{p}$	–	3.8 ± 1.0	0.09
Total BR (Exclusive)		302 ± 37	7.0
Total BR (Resonance + Exclusive)		482 ± 38	11.2

even when HO QCD corrections and gluon mass effects were included. The procedure adopted was then to fix the ratio $\Gamma(J/\psi \to \gamma\eta')/\Gamma(J/\psi \to \gamma\eta)$ to the measured value 5.0 [3], and perform fits treating the ratio

$$R_{\eta'} = \Gamma(J/\psi \to \gamma\eta')/\Gamma(J/\psi \to \gamma \text{ continuum})$$

as a free parameter, which include the η' and η contributions at the appropriate z values of 0.904 and 0.969, respectively. Here "γ continuum" refers to Eq. (2.8), including also gluon mass effects and the Photiadis HO QCD correction. The other two parameters in the fit are an overall normalization constant and the effective gluon mass m_g. The method used to fold in the experimental resolution function is described in the Appendix. As shown in Table IV, attempting to fit the spectrum without explicitly introducing the η' and η contributions (i.e., with $R_{\eta'} = 0$) leads to an unacceptably low confidence level (C.L.) of 3×10^{-3}. However, including their contributions, good fits are obtained for all three spectra with consistent values of $R_{\eta'}$. Their weighted average is

$$R_{\eta'} = 0.0754 \pm 0.0070.$$

The Mark II and Mark II(cascade) spectra yield consistent values of m_g around 720 MeV, but the Mark II(conversion) spectrum gives a significantly lower (5.8σ) value of 597 MeV, indicating some systematic difference in the latter measurement. The weighted average value of $R_{\eta'}$ corresponds to

TABLE IV. Results of fits to determine the fractions of $J/\psi \rightarrow \gamma\eta', \gamma\eta$ in J/ψ radiative decays.

η' fraction	η fraction	m_g	χ^2_{min}	CL
		Mark II (25 DOF)		
0.0	0.0	0.610 ± 0.015	51.7	2×10^{-3}
$0.074^{+0.006}_{-0.011}$	0.015	0.720 ± 0.012	17.5	0.86
		Mark II cascade (25 DOF)		
$0.078^{+0.009}_{-0.011}$	0.016	$0.722^{+0.019}_{-0.017}$	18.3	0.79
		Mark II conversion (22 DOF)		
$0.073^{+0.016}_{-0.010}$	0.015	0.597 ± 0.019	20.0	0.58

$$\mathrm{BR}(J/\psi \rightarrow \gamma + \text{continuum} + \eta + \eta') = 0.063 \pm 0.0070,$$

which may be compared to the summed branching ratio of all channels reported in Table III of 0.0482 ± 0.0038. So it is estimated that 76% of all J/ψ radiative decays to light hadrons are contributed by the resonances and exclusive channels listed in Table III.

The results of fits to the three inclusive photon spectra, including the exclusive η' and η contributions, estimated using the weighted average value of $R_{\eta'}$ obtained above, without including gluon mass effects, are presented in Table V and Fig. 3. No acceptable fits are obtained, even after the inclusion of of both relativistic and HO QCD corrections. The best confidence levels obtained for the fits to the Mark II, Mark II(cascade), and Mark II(conversion) spectra are

TABLE V. Results of fits with $m_g = 0$ to J/ψ inclusive photon spectra. LO denotes the lowest order QCD prediction [Eq. (3.1)]. Rel. Corr^n includes relativistic corrections calculated according to Eq. (2.8). QCD(P) and QCD(K) denote, respectively, the Photiadis [17] and Krämer [14] HO QCD corrections. QCD(P×K) means that both corrections are applied.

Fitted model	χ^2_{min}	C.L.
	Mark II (27 DOF)	
LO	666	$<10^{-30}$
Rel. Corr^n	336	$<10^{-30}$
Rel. Corr^n, QCD(P)	279	$<10^{-30}$
Rel. Corr^n, QCD(K)	253	$<10^{-30}$
Rel. Corr^n, QCD(P×K)	224	$<10^{-30}$
	Mark II cascade (26 DOF)	
LO	348	$<10^{-30}$
Rel. Corr^n	183	1.5×10^{-25}
Rel. Corr^n, QCD(P)	153	5.9×10^{-20}
Rel. Corr^n, QCD(K)	136	7.3×10^{-17}
Rel. Corr^n, QCD(P×K)	121	3.3×10^{-14}
	Mark II conversion (24 DOF)	
LO	198	$<2.5 \times 10^{-29}$
Rel. Corr^n	80.9	4.4×10^{-25}
Rel. Corr^n, QCD(P)	66.3	7.8×10^{-6}
Rel. Corr^n, QCD(K)	50.8	1.1×10^{-3}
Rel. Corr^n, QCD(P×K)	45.0	5.8×10^{-3}

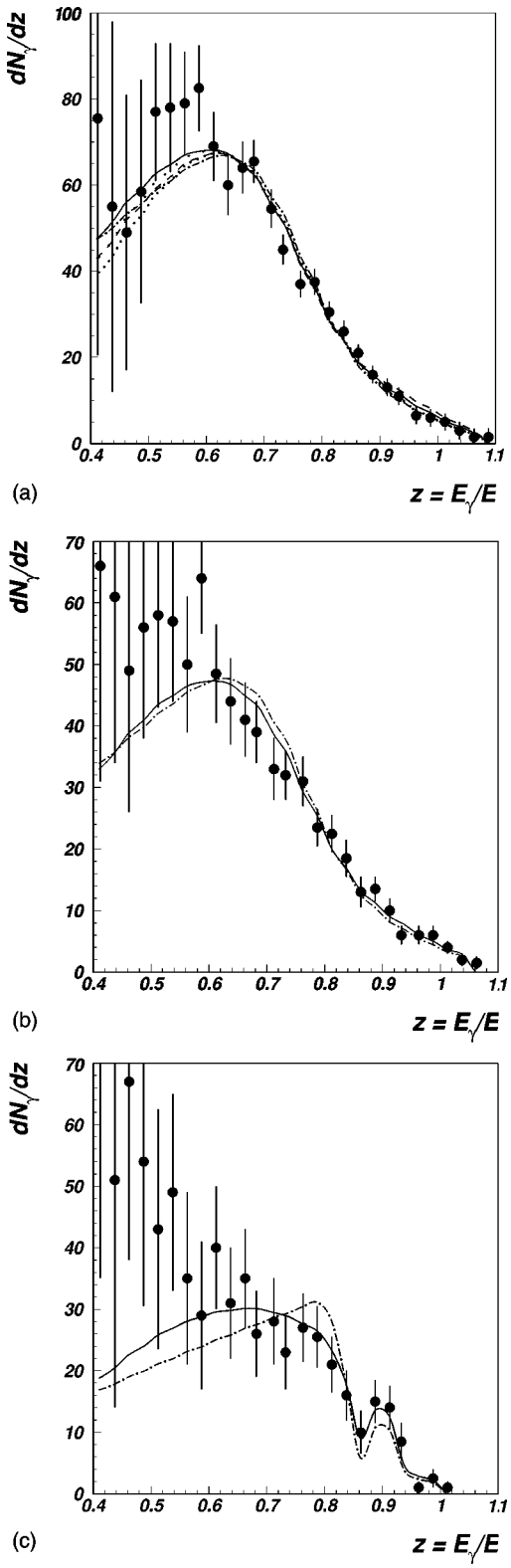

FIG. 4. Fits, for the effective gluon mass m_g, to inclusive photon spectra in J/ψ decays. Mark II (top left), Mark II cascade (top right), Mark II conversion (bottom). Fit curves are defined as in Fig. 3.

TABLE VI. Results of fits with variable m_g to J/ψ inclusive photon spectra. LW denotes gluon mass corrections calculated according to the calculations of Liu and Wetzel [39]. Relativistic and HO QCD corrections are defined as in Table V.

Fitted model	m_g (GeV)	χ^2_{min}	C.L.
	Mark II (26 DOF)		
LW	0.734 ± 0.010	24.6	0.54
LW, Rel. Corr^n	$0.740^{+0.009}_{-0.012}$	22.6	0.66
LW, Rel. Corr^n QCD(P)	$0.721^{+0.010}_{-0.009}$	17.5	0.89
LW, Rel. Corr^n QCD(K)	$0.665^{+0.014}_{-0.013}$	19.9	0.80
LW, Rel. Corr^n QCD(P×K)	$0.653^{+0.018}_{-0.015}$	16.9	0.91
	Mark II cascade (25 DOF)		
LW	$0.737^{+0.015}_{-0.018}$	24.4	0.50
LW, Rel. Corr^n	0.740 ± 0.017	21.9	0.64
LW, Rel. Corr^n QCD(P)	0.719 ± 0.019	18.4	0.82
LW, Rel. Corr^n QCD(K)	0.667 ± 0.021	22.7	0.60
LW, Rel. Corr^n QCD(P×K)	0.655 ± 0.021	20.0	0.75
	Mark II conversion (23 DOF)		
LW	$0.623^{+0.013}_{-0.016}$	31.6	0.11
LW, Rel. Corr^n	$0.607^{+0.015}_{-0.017}$	23.9	0.41
LW, Rel. Corr^n QCD(P)	$0.598^{+0.018}_{-0.017}$	19.9	0.65
LW, Rel. Corr^n QCD(K)	$0.537^{+0.025}_{-0.030}$	22.5	0.49
LW, Rel. Corr^n QCD(P×K)	$0.526^{+0.027}_{-0.029}$	20.3	0.62

$<10^{-30}$, 3.3×10^{-14}, and 5.8×10^{-3}, respectively. Although, as expected from Fig. 1, the shape of the spectrum is drastically modified by the relativistic correction, the change in shape, though qualitatively in the right direction, is by far not enough to explain the observed spectrum shape. As can be seen in Fig. 3(a), the estimated effects of HO QCD corrections are even smaller than those of the relativistic correction.

A similar series of fits, but including gluon mass effects, is presented in Table VI and Fig. 4. Good fits are obtained in all cases, and it can be seen that the inclusion of relativistic and HO QCD corrections has only a minor effect on the fitted values of m_g. For example, in the case of the largest statistics data sample (Mark II), introducing the relativistic correction increases the fitted value of m_g of 734 MeV by only 6 MeV. Further applying either the Photiadis or Krämer HO QCD corrections gives further shifts of -19 MeV or -75 MeV, respectively, in the fitted m_g value. In fact because of the relatively large value of m_g as compared to $M_{J/\psi}$, it is to be expected, as mentioned previously, that HO QCD corrections will be much reduced by phase-space and propagator suppression effects. Choosing then the fit with relativistic and the smallest (Photiadis) HO QCD correction as best estimate yields the result

$$m_g = 0.721^{+0.010+0.013}_{-0.009-0.068} \quad \text{GeV} \quad (J/\psi)$$

where the first error is statistical (from the fit to the Mark II spectrum) and the second is systematic, conservatively estimated from the full spread of the different fit results to the Mark II data given in Table VI. In view of the size of this systematic error in the Mark II value, and the large observed systematic shift in m_g obtained with the Mark II(conversion) spectrum, no significant improvement in the knowledge of m_g is expected by combining the results of the fits to the three spectra. The less precise values provided by the Mark II(cascade) and Mark II(conversion) data should then be considered as consistency checks.

TABLE VII. Results of fits with $m_g=0$ to Υ inclusive photon spectra. See Table V for the definitions of the different fits.

Fitted model	χ^2_{min}	C.L.
	CUSB (11 DOF)	
LO	30.2	$<1.5\times10^{-3}$
Rel. Corr^n	10.9	0.45
Rel. Corr^n, QCD(P)	14.7	0.2
Rel. Corr^n, QCD(K)	13.0	0.29
Rel. Corr^n, QCD(P×K)	21.3	0.03
	ARGUS (19 DOF)	
LO	95.3	3.8×10^{-12}
Rel. Corr^n	62.6	1.5×10^{-6}
Rel. Corr^n, QCD(P)	44.7	7.5×10^{-4}
Rel. Corr^n, QCD(K)	49.8	1.4×10^{-4}
Rel. Corr^n, QCD(P×K)	37.6	6.7×10^{-3}
	Crystal Ball (14 DOF)	
LO	51.9	2.9×10^{-6}
Rel. Corr^n	31.6	4.6×10^{-3}
Rel. Corr^n, QCD(P)	22.4	0.071
Rel. Corr^n, QCD(K)	24.6	0.039
Rel. Corr^n, QCD(P×K)	18.9	0.17
	CLEO2 (22 DOF)	
LO	90.7	2.6×10^{-10}
Rel. Corr^n	56.9	6.3×10^{-5}
Rel. Corr^n, QCD(P)	32.1	0.076
Rel. Corr^n, QCD(K)	48.8	8.5×10^{-4}
Rel. Corr^n, QCD(P×K)	29.5	0.131

It may be noted that the exclusive η' signal is clearly seen in the Mark II(conversion) spectrum shown in Figs. 3(c) and 4(c). The shape of the observed peak is well described in Fig. 4(c) by the fit including the relativistic and Photiadis HO QCD corrections, and the experimental resolution function given in Table II. This agreement gives an important cross-check on the method used here (see the Appendix) to fold in the experimental resolution effects.

In order to study the relative importance of phase-space effects and longitudinal gluon contributions in the gluon mass fits, the fit to the Mark II data, including both the relativistic and the Photiadis HO QCD corrections, is repeated setting $m_g=0$ in the function $f_0(z,x_2,m_g)$ of Eq. (4.7), thus

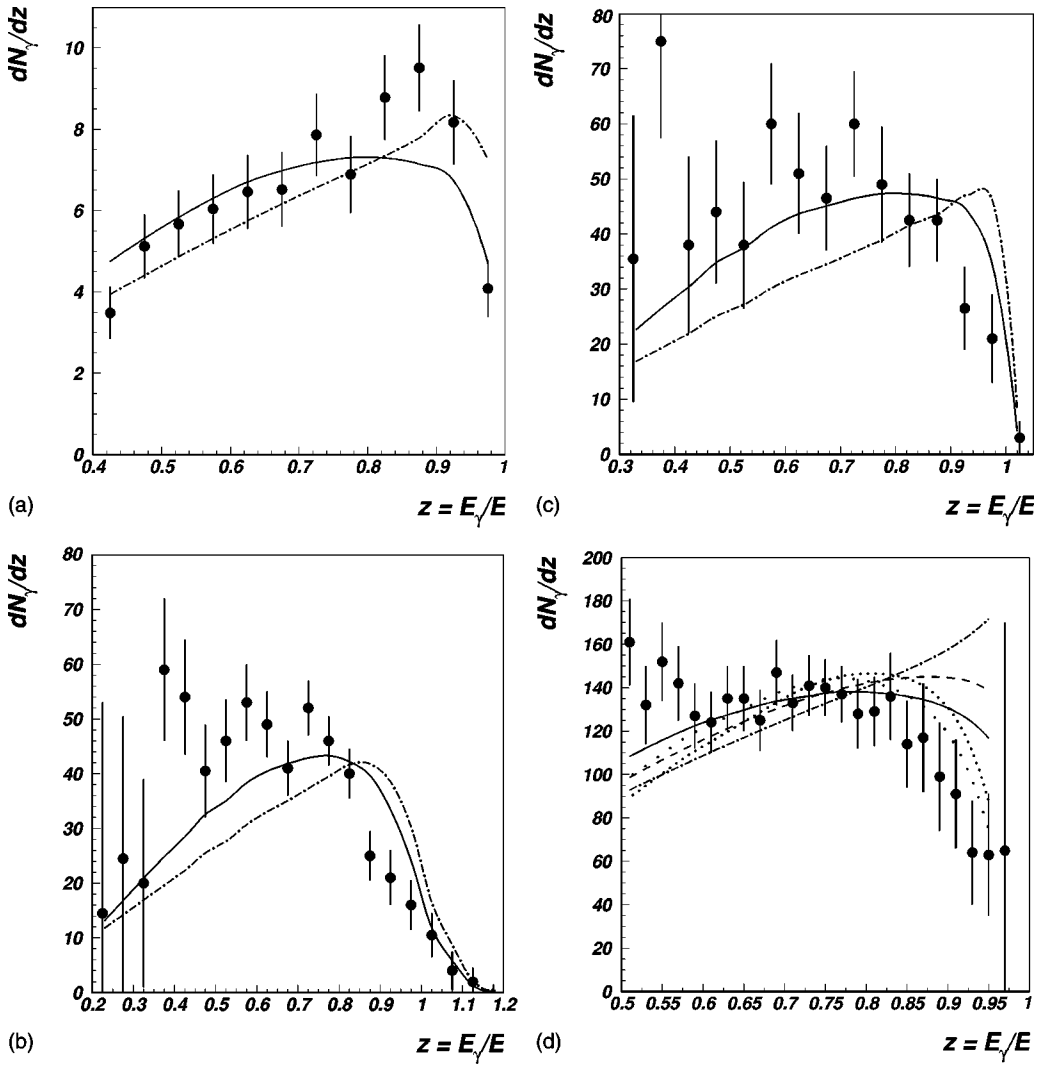

FIG. 5. Fits, assuming $m_g=0$, to inclusive photon spectra in Υ decays: CUSB (top left), ARGUS (top right), Crystal Ball (bottom left), CLEO2 (bottom right). Fit curves are defined as in Fig. 3.

removing the longitudinal contributions. A very good fit is still obtained (confidence level 0.94) with $m_g=0.682+0.010-0.013$ GeV. This is only 5.4% lower than the value $m_g=0.721+0.010-0.009$ GeV obtained including the longitudinal contributions. Thus the gluon mass correction is dominated by phase-space effects.

VI. THE DECAY $\Upsilon\rightarrow\gamma X$

Five different experiments have measured the inclusive photon spectrum in Υ decays: CUSB [41], CLEO [42], ARGUS [43], Crystal Ball [44], and CLEO2 [45]. The CLEO measurement, which, like Crystal Ball, ARGUS, and CLEO2, but unlike CUSB, is in good agreement with the Field prediction, is not analyzed in the present paper as no efficiency corrected spectrum was provided.

Unlike for the case of the J/ψ, no positive evidence has been found for the exclusive production of single resonances in the radiative decays of the Υ [3]. The efficiency corrected inclusive photon spectra measured by CUSB, ARGUS, Crystal Ball, and CLEO2 have therefore been directly fitted to the relativistically corrected spectrum Eq. (2.8), possibly also including HO QCD corrections as discussed in Sec. III and gluon mass effects as described in Sec. IV. Experimental resolution effects are included in the same way as for the fits to the J/ψ decays described above. The photon energy resolutions of the different experiments are given in Table II. Results of fits assuming a vanishing effective gluon mass are presented in Table VII and Fig. 5, while fits to m_g and an overall normalization constant yield the results shown in Table VIII and Fig. 6.

As can be seen in Figs. 5 and 6, the CUSB spectrum differs markedly in shape from those of the later ARGUS, Crystal Ball, and CLEO2 experiments. The suppression of the end-point region, relative to the LO QCD prediction (the dash-dotted curves), is much reduced. The results of the fits to the CUSB data should be treated with caution as, unlike the other experiments, the published errors on the photon spectrum are purely statistical. A relatively large systematic error is expected (as found in the other experiments) from the π^0/γ separation procedure, especially at lower values of z.

Considering first the fits with $m_g=0$ in Table VII, it can

TABLE VIII. Results of fits with variable m_g to Υ inclusive photon spectra. The descriptions of the different fitted models are the same as in Table VI.

Fitted model	m_g (GeV)	χ^2_{min}	C.L.
	CUSB (10 DOF)		
LW	0.66 ± 0.08	5.2	0.88
LW, Rel. Corr^n	0.64 ± 0.09	6.1	0.81
LW, Rel. Corr^n QCD(P)	0.54 ± 0.12	13.1	0.22
LW, Rel. Corr^n QCD(K)	$0.16^{+0.17}_{-0.16}$	12.6	0.25
LW, Rel. Corr^n QCD(P×K)	$0.15^{+0.18}_{-0.15}$	21.0	0.021
	ARGUS (18 DOF)		
LW	$1.39^{+0.08}_{-0.10}$	27.3	0.074
LW, Rel. Corr^n	1.39 ± 0.10	28.8	0.051
LW, Rel. Corr^n QCD(P)	$1.27^{+0.11}_{-0.12}$	23.3	0.18
LW, Rel. Corr^n QCD(K)	$1.19^{+0.10}_{-0.12}$	34.4	0.011
LW, Rel. Corr^n QCD(P×K)	$1.06^{+0.13}_{-0.16}$	28.8	0.05
	Crystal Ball (13 DOF)		
LW	$1.21^{+0.10}_{-0.09}$	21.5	0.064
LW, Rel. Corr^n	$1.21^{+0.10}_{-0.11}$	22.2	0.052
LW, Rel. Corr^n QCD(P)	$1.14^{+0.12}_{-0.16}$	18.0	0.16
LW, Rel. Corr^n QCD(K)	$0.90^{+0.19}_{-0.40}$	23.5	0.036
LW, Rel. Corr^n QCD(P×K)	No χ^2_{min}	—	—
	CLEO2 (21 DOF)		
LW	1.27 ± 0.07	29.5	0.103
LW, Rel. Corr^n	$1.25^{+0.08}_{-0.07}$	30.4	0.08
LW, Rel. Corr^n QCD(P)	$1.15^{+0.08}_{-0.09}$	16.9	0.72
LW, Rel. Corr^n QCD(K)	$1.03^{+0.09}_{-0.12}$	34.5	0.032
LW, Rel. Corr^n QCD(P×K)	$0.90^{+0.11}_{-0.13}$	22.5	0.37

be seen that the LO spectrum is ruled out, individually, by all four experiments. Inclusion of the relativistic correction with $\langle v^2 \rangle = 0.09$ gives a good description of the CUSB data but is ruled out with a confidence level of less than 0.5% by each of the other experiments. The best overall description is given by combining the relativistic and Photiadis HO QCD corrections. Low, but acceptable, confidence levels of 0.2, 0.071, and 0.076 are found for the fits to CUSB, Crystal Ball, and CLEO2 data, respectively. Only the ARGUS spectrum (C.L. $= 7.5 \times 10^{-4}$) is inconsistent with this hypothesis. However, combining the fits to all four experiments gives $\chi^2/\mathrm{DOF} = 114/66$ (C.L. $= 2.3 \times 10^{-4}$).

For ARGUS, Crystal Ball, and CLEO2 the best fits are given by including both the Photiadis and Krämer HO QCD corrections. The combined fit gives, however, $\chi^2/\mathrm{DOF} = 86/66$ (C.L. $= 4.7 \times 10^{-3}$). Thus no consistent overall description of the data is found for $m_g = 0$.

When the effective gluon mass m_g is included as a fit parameter it can be seen (Table VIII) that fits with confidence levels $> 1\%$ are found for all fit hypotheses and all experimental spectra. However, the ARGUS, Crystal Ball, and CLEO2 data give consistent values of m_g in the range 0.9–1.4 GeV, whereas significantly lower values 0.15–0.66 GeV are found in the fits to the CUSB spectrum. Because of this discrepancy and the neglect of (potentially large) systematic errors in the latter experiment, only the results from the three most recent experiments are used to obtain the average value of m_g quoted below. For these experiments the best overall fit is given (as in the case $m_g = 0$) by including both the relativistic and the Photiadis HO QCD correction. This yields, for the weighted average value of the effective gluon mass

$$m_g = 1.18 \pm 0.06 \ \text{GeV},$$

where the error quoted is derived from fit errors of the different experiments. Performing a fit to the ARGUS, Crystal Ball, and CLEO2 spectra, with m_g fixed at the above value, and varying only the normalization constants of the fitted curves gives a good overall fit with $\chi^2/\mathrm{DOF} = 59.0/55$ (C.L. $= 0.33$). Making the same type of fit but including CUSB data leads to $\chi^2/\mathrm{DOF} = 121.0/66$ (C.L. $= 4.3 \times 10^{-5}$). The published CUSB data are therefore clearly inconsistent with the value of m_g favored by ARGUS, Crystal Ball, and CLEO2. This apparent inconsistency of the CUSB measurement, is, however, very sensitive to the error assignement of the data. Increasing the quoted (purely statistical) errors by a constant factor of 1.5 to account for systematic effects modifies the last fit result quoted above to $\chi^2/\mathrm{DOF} = 89.0/66$ (C.L. $= 0.031$). The CUSB measurement is now marginally consistent with the average of the three other experiments.

The theoretical systematic error on m_g is estimated in the same way as for J/ψ decays. This gives

$$m_g = 1.18 \pm 0.06^{+0.07}_{-0.28} \ \text{GeV} \quad (\Upsilon),$$

where the first error is experimental and the second is a conservatively estimated theoretical error that includes the full range of relativistic and HO QCD corrections in the fits to the CLEO2 data in Table VIII.

To investigate the importance of the effects of longitudinal gluon polarization states for the case of the Υ, a fit is made to the CLEO2 data including relativistic and the Photiadis HO QCD corrections, with $m_g = 0$ in the function f_0 of Eq. (4.7). The fit gives $m_g = 1.10 + 0.08 - 0.09$ GeV with $\chi^2/\mathrm{DOF} = 13.1/21$ (C.L. $= 0.91$) to be compared with $m_g = 1.15 + 0.08 - 0.09$ GeV with $\chi^2/\mathrm{DOF} = 16.9/21$(C.L. $= 0.70$) when longitudinal gluon contributions are included in f_0. As in the case of the J/ψ, longitudinal gluon states give only a small effect; they increase the fitted value of m_g by only 4.5%.

Finally in this section we make a few remarks on the CLEO measurement [42], which is not included in the

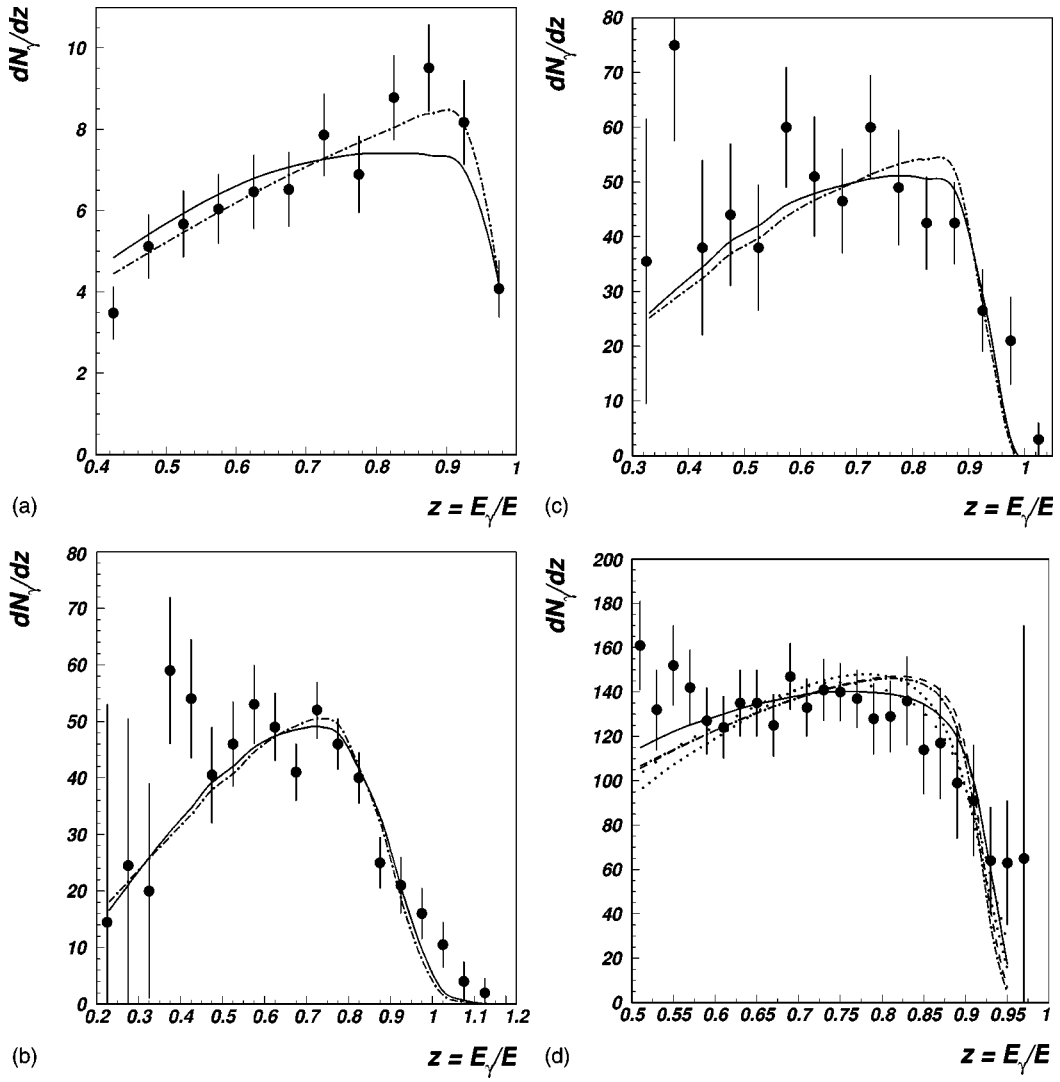

FIG. 6. Fits, for the effective gluon mass m_g, to inclusive photon spectra in Υ decays: CUSB (top left), ARGUS (top right), Crystal Ball (bottom left), CLEO2 (bottom right). Fit curves are defined as in Fig. 3.

present analysis. Relativistic corrections were not taken into account in the theoretical predictions, which were suitably modified to account for detector acceptance and resolution effects before comparison with the (uncorrected) experimental data. Fitting the LO QCD, Photiadis, and Field spectra to the data yields χ^2 of 14.2, 10.0, and 8.1, respectively, for 11 degrees of freedom [42]. The corresponding respective confidence levels are 0.22, 0.46, and 0.70. Although the Field model is slightly favored, all the fits have acceptable confidence levels and no distinction between the different theoretical models is possible from this measurement.

VII. DETERMINATIONS OF $\alpha_S(M_Q)$

The strong coupling constant $\alpha_s(m_Q)$ may be determined from the experimental measurements of the branching ratio:

TABLE IX. Experimental branching ratios used to determine $\alpha_s(m_Q)$.

Branching ratio	Experimental value	Reference
$\Gamma(J/\psi\rightarrow\text{hadrons})/\Gamma_{J/\psi}$	0.632 ± 0.022	[3]
$\Gamma(J/\psi\rightarrow\gamma+\text{hadrons})/\Gamma_{J/\psi}$	0.0624 ± 0.0067	This paper
$R'_{J/\psi}$	10.13 ± 1.14	Ratio of above
R'_Υ	33.33 ± 2.44	ARGUS [43]
R'_Υ	37.04 ± 6.17	Crystal Ball [44]
R'_Υ	36.36 ± 2.11	CLEO2 [45]
R'_Υ	35.46 ± 1.51	Weighted average

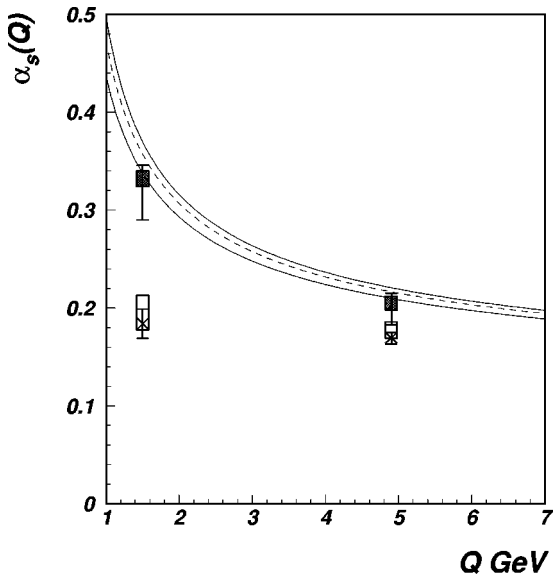

FIG. 7. $\alpha_s(m_c)$ and $\alpha_s(m_b)$ values obtained from measurements of $R'_{J/\psi}$ and R'_{Υ} compared to the world average value (dashed curve with $\pm 1\sigma$ limits indicated by the solid curves) from Ref. [3]. The crosses with error bars show values obtained assuming $m_g=0$ and $\mu/m_Q=1.0$. The effect of varying the renormalization scale in the range $0.6<\mu/m_Q<2.0$ is indicated by the vertical boxes. The square points with error bars are obtained by applying full gluon mass corrections with $m_g=0.721$ GeV for the J/ψ and $m_g=1.18$ GeV for the Υ with $\mu/m_Q=1.0$. NLO QCD corrections are applied in all cases.

$$R'_V \equiv \frac{\Gamma(V\to\text{hadrons})}{\Gamma(V\to\gamma+\text{hadrons})} \tag{7.1}$$

where V denotes a vector heavy quarkonium ground state (J/ψ or Υ). Use of R'_V has the advantage, as compared with other branching ratios sensitive to α_s [for example, $R_V \equiv \Gamma(V\to\text{hadrons})/\Gamma(V\to l^+l^-)$] that relativistic corrections cancel in the approximation used in the present paper.

In Eq. (7.1) the process "$V\to\gamma+$hadrons" is understood to be the heavy quark annihilation process into light hadrons, for which the lowest order QCD process is $V\to\gamma gg$. Thus the nonannihilation process $V\to\gamma\eta_Q$, where η_Q is the lowest lying pseudoscalar heavy quarkonium ground state, is not included. Similarly, "$V\to$hadrons" is understood to be the direct (strong interaction) process for which the lowest order QCD process is $V\to ggg$. The contribution of the radiative process $V\to\gamma^\star\to q\bar{q}\to$hadrons (branching ratio 17% for the J/ψ) is, therefore, not included.

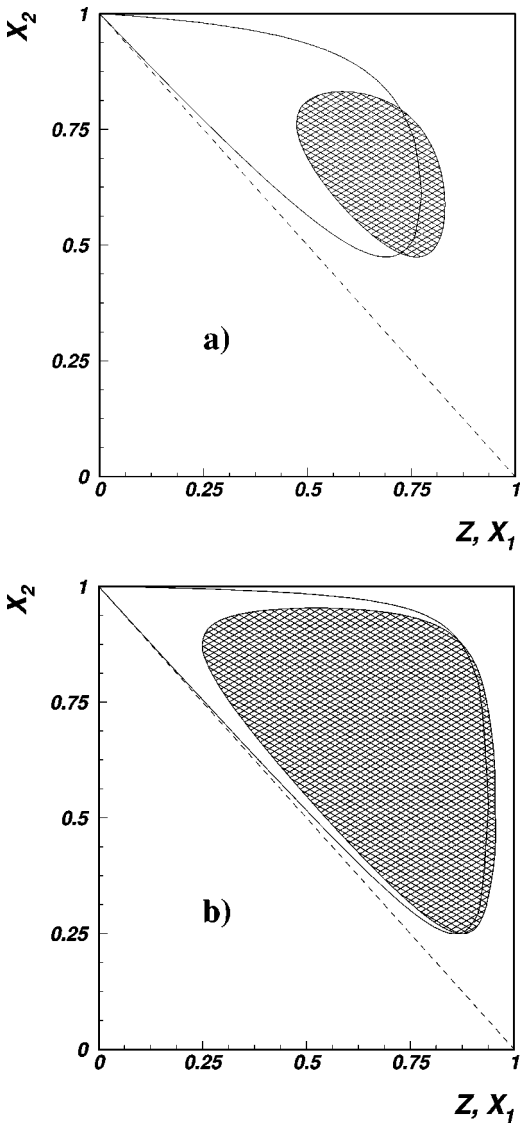

FIG. 8. Allowed regions of the Dalitz plots for $V\to\gamma gg$ (open areas) and $V\to ggg$ (cross-hatched areas), corresponding to the effective gluon mass values 0.721 GeV (J/ψ) (a) and 1.18 GeV (Υ) (b). For vanishing effective gluon mass, the full areas above the dotted lines are kinematically allowed.

TABLE X. $\alpha_s(m_Q)$ values obtained neglecting gluon mass corrections for different choices of the renormalization scale μ. Δ(PDG) is the difference from the Particle Data Group (PDG) [3] average values: $\alpha_s(m_c)=0.357^{+0.013}_{-0.019}$, $\alpha_s(m_b)=0.217^{+0.004}_{-0.007}$. "Deviation" is Δ(PDG) divided by its error.

μ/m_Q	0.6	1.0	2.0
$\alpha_s(m_c)$	0.178 ± 0.011	0.184 ± 0.015	0.213 ± 0.023
$\Delta(PDG)$	-0.179 ± 0.022	-0.173 ± 0.024	-0.144 ± 0.03
Deviation(σ)	-8.1	-7.2	-4.8
$\alpha_s(m_b)$	0.169 ± 0.005	0.169 ± 0.006	0.186 ± 0.008
$\Delta(PDG)$	-0.048 ± 0.008	-0.048 ± 0.009	-0.031 ± 0.01
Deviation(σ)	-6.0	-5.3	-3.0

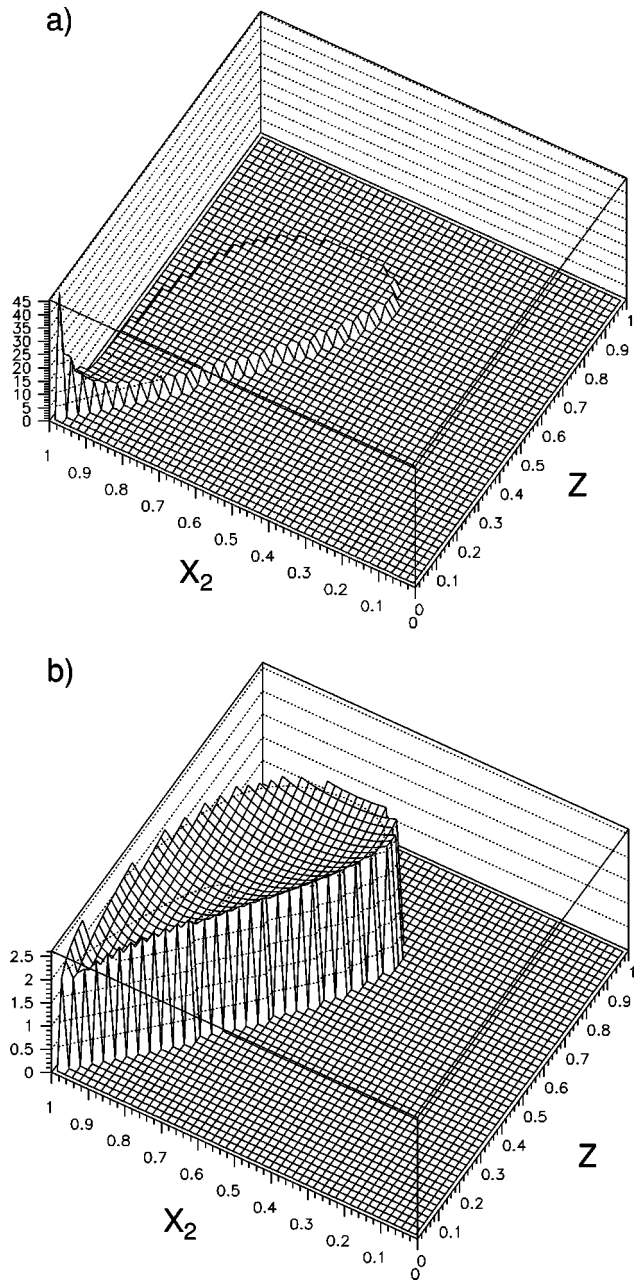

FIG. 9. The effect of gluon mass corrections ($m_g = 0.721$ GeV) on the differential decay rate $d\Gamma/dzdx_2$ [Eq. (4.1)] for $J/\psi \to \gamma gg$ decays. (a) Phase-space effects only; (b) inclusion also of longitudinal gluon polarization states.

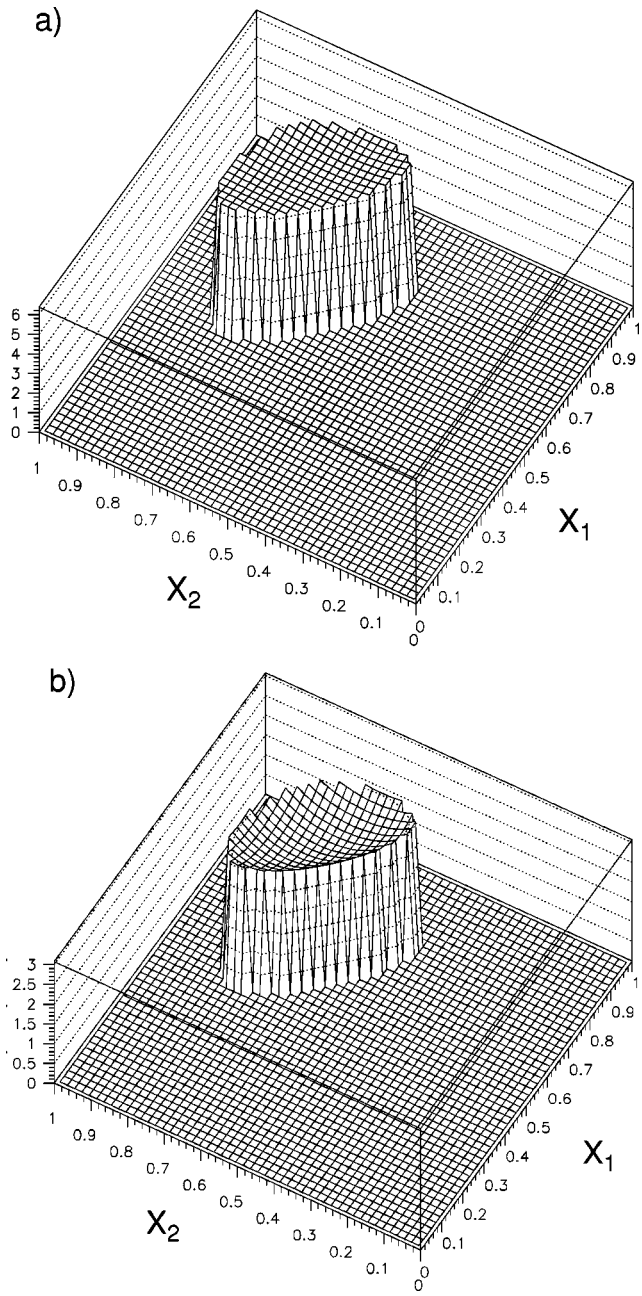

FIG. 10. The effect of gluon mass corrections ($m_g = 0.721$ GeV) on the differential decay rate $d\Gamma/dx_1dx_2$ [Eq. (7.6)] for $J/\psi \to ggg$ decays. (a) Phase-space effects only; (b) inclusion also of longitudinal gluon polarization states.

The experimental branching ratios used here to extract $\alpha_s(m_Q)$ are summarized in Table IX. For the J/ψ the branching ratio $\Gamma(J/\psi \to \gamma + \text{hadrons})/\Gamma_{J/\psi}$, where $\Gamma_{J/\psi}$ denotes the total width of the J/ψ, is obtained from the fits to the branching ratio $R_{\eta'}$ presented in Table IV. The measured exclusive branching ratio into $\gamma\eta'$ [3] is used to derive, from $R_{\eta'}$, the branching fraction for the "γ continuum" (see Sec. V above). The measured exclusive $\gamma\eta$ and $\gamma\eta'$ fractions are then added to the "γ continuum" fraction to give the full branching fraction into γ+hadrons quoted in Table IX. The errors on this quantity are derived from that on the weighted average value of $R_{\eta'}$ and the experimental $\gamma\eta$ and $\gamma\eta'$ fractions [3]. The branching fraction $\Gamma(J/\psi \to \text{hadrons})/\Gamma_{J/\psi}$ is derived from the total hadronic width of the J/ψ given in Ref. [3] by subtracting the contribution [3] of the process $J/\psi \to \gamma^\star \to q\bar{q} \to$ hadrons.

In the case of the Υ measurements, the branching ratio R'_Υ was directly measured by CUSB, CLEO, ARGUS, Crystal Ball, and CLEO2. The values of R'_Υ obtained by the last three of these experiments are reported in Table IX. In all cases the extrapolation of the measured photon spectrum to $z=0$ was done using the Field theoretical spectrum. As will be shown below, the shape of this spectrum is in good agree-

ment with the fit curves obtained in the present paper, which take into account relativistic corrections and explicit gluon mass effects at the Born level. This shape is little affected by including HO QCD corrections according to Ref. [17] and/or Ref. [14]. To extract $\alpha_s(m_b)$, the weighted average (also reported in Table IX) of the R'_Υ measurements of ARGUS, Crystal Ball, and CLEO2 is used.

Consistent results for R'_Υ were found by CUSB, 33.4 ± 6.6, and CLEO (using the Field spectrum), 39.4 ± 3.6. Since, however, the shape of the inclusive photon spectrum measured by CUSB is inconsistent with those measured by the other four experiments, and the analysis of the CLEO photon spectrum could not be performed, these two measurements are omitted from the R'_Υ average used here to determine $\alpha_s(m_b)$. Thus, the α_s analysis is performed using only data from experiments for which a consistent determination of the effective gluon mass was possible. Including also the CUSB and CLEO measurements in the weighted average of R'_Υ gives the value 35.94 ± 1.36, which differs by only 0.35σ from the weighted average of ARGUS, Crystal Ball, and CLEO2 quoted in the last row of Table IX.

Taking into account NLO QCD radiative corrections [46] as well as gluon mass corrections, $\alpha_s(m_Q)$ may be derived from the formulas

$$R'_{J/\psi} = \frac{5\alpha_s(\mu)}{16\alpha} \frac{f_{ggg}}{f_{\gamma gg}} \frac{\left[1 + \frac{\alpha_s(\mu)}{\pi}\left(\frac{3}{2}\beta_0 \ln\frac{\mu}{m_c} - 3.74\right)\right]}{\left[1 + \frac{\alpha_s(\mu)}{\pi}\left(\beta_0 \ln\frac{\mu}{m_c} - 6.68\right)\right]}, \tag{7.2}$$

$$R'_\Upsilon = \frac{5\alpha_s(\mu)}{4\alpha} \frac{f_{ggg}}{f_{\gamma gg}} \frac{\left[1 + \frac{\alpha_s(\mu)}{\pi}\left(\frac{3}{2}\beta_0 \ln\frac{\mu}{m_b} - 4.90\right)\right]}{\left[1 + \frac{\alpha_s(\mu)}{\pi}\left(\beta_0 \ln\frac{\mu}{m_b} - 7.45\right)\right]}. \tag{7.3}$$

Here β_0 is the one-loop QCD beta function coefficient

$$\beta_0 = 11 - \frac{2n_f}{3}$$

where the number of active quark flavors, n_f, is taken to be 3 for the J/ψ and 4 for the Υ. The values of the heavy quark masses are assumed to be $m_c = 1.5$ GeV and $m_b = 4.9$ GeV. The parameter μ is an arbitary renormalization scale, and $f_{ggg}, f_{\gamma gg}$ are correction factors taking into account gluon mass effects. As previously pointed out, relativistic corrections cancel in the ratio R'_V. For any given value of the renormalization scale μ, Eqs. (7.2) or (7.3) are solved for $\alpha_s(\mu)$. The corresponding value of $\alpha_s(m_Q)$ is then found by use of the one-loop QCD evolution formula:

$$\frac{1}{\alpha_s(m_Q)} = \frac{1}{\alpha_s(\mu)} - \frac{\beta_0}{2\pi} \ln\frac{\mu}{m_Q}. \tag{7.4}$$

Setting $f_{ggg} = f_{\gamma gg} = 1$ (i.e., neglecting gluon mass corrections) and choosing the values[6] $\mu/m_Q = 0.6$, 1.0, and 2.0 yields the values of $\alpha_s(m_c)$ and $\alpha_s(m_b)$ reported in Table X. It can be seen that there is poor agreement with the world average values [3]:

$$\alpha_s(1.5 \text{ GeV}) = 0.357^{+0.013}_{-0.019},$$
$$\alpha_s(4.9 \text{ GeV}) = 0.217^{+0.004}_{-0.007}.$$

These are calculated using Eq. (9.5) of Ref. [47] and correspond to four active quark flavors. Matching to the five-flavor region where $\Lambda^{(5)} = 219^{+25}_{-23}$ MeV [corresponding to the world average value $\alpha_s(M_Z) = 0.119 \pm 0.002$] is done using Eq. (9.7) of Ref. [47] at a matching scale of 4.3 GeV. For both the J/ψ and the Υ the best agreement is found for $\mu/m_Q = 2.0$, but the respective deviations are still 4.8σ and 3.0σ. Figure 7 shows a comparison of the $\alpha_s(m_c)$ and $\alpha_s(m_b)$ values quoted in Table X for $\mu/m_Q = 1.0$ with the present world average value of $\alpha_s(Q)$ [3].

The gluon mass correction factors are calculated by integrating the differential distributions of gluon and photon energies of the decay processes $V \to \gamma gg$ or $V \to ggg$ over the kinematically allowed regions of their respective Dalitz plots. For $V \to \gamma gg$ it is convenient to use the photon spectrum given by integrating Eq. (4.1) over the gluon energies [39]:

$$\frac{1}{\Gamma_0}\frac{d\Gamma}{dz} = \frac{1}{\pi^2 - 9}\left[\frac{x_+ - x_-}{z^2} + \frac{\ln(x_+/x_-)}{z^2(-2+4\eta+z)^3}[8(2\eta-1)^2(2-4\eta+7\eta^2) + 8(2\eta-1)(5-12\eta+10\eta^2+2\eta^3)z + 2(2\eta - 1)(-17+10\eta+6\eta^2)z^2 + 2(-5+2\eta+2\eta^2)z^3] + \frac{(1/x_- - 1/x_+)}{z^2(-2+4\eta+z)^2}[4(2\eta-1)^2(1+3\eta^2) + 4(2\eta-1)(3 - 4\eta+2\eta^2+2\eta^3)z + 2(7-18\eta+10\eta^2+10\eta^3)z^2 + 4(2+\eta)(2\eta-1)z^3 + (2+\eta)z^4]\right], \tag{7.5}$$

where

[6]Equations (7.2) and (7.3) have no real solution for $\alpha_s(\mu)$ when $\mu/m_Q = 0.5$.

$$x_{\pm}=1-2\eta-\frac{z}{2}\left[1\mp\sqrt{1-\frac{4\eta}{1-z}}\right].$$

For the decays $V\to ggg$ a two-dimensional integration is performed over the distribution [39]:

$$\begin{aligned}\frac{1}{\Gamma_0}\frac{d\Gamma}{dx_1dx_2dx_3}=&\frac{1}{(\pi^2-9)}\frac{1}{(x_1')^2(x_2')^2(x_3')^2}\left[\frac{16}{3}\eta(1-3\eta)^2\left(1-\frac{51}{8}\eta-\frac{15}{4}\eta^2\right)\right.\\&+((x_1')^2+(x_2')^2+(x_3')^2)(1-14\eta+48\eta^2+25\eta^3)\\&-2[(x_1')^3+(x_2')^3+(x_3')^3]\left(1-\frac{17}{3}\eta-3\eta^2\right)\\&\left.+[(x_1')^4+(x_2')^4+(x_3')^4]\left(1+\frac{\eta}{2}\right)\right].\end{aligned}\tag{7.6}$$

The allowed phase-space region is

$$2=x_1+x_2+x_3,\tag{7.7}$$

$$2\sqrt{\eta}\leqslant x_1\leqslant 1-3\eta,\tag{7.8}$$

$$x_2^{min}\leqslant x_2\ \leqslant x_2^{max},\tag{7.9}$$

$$x_2^{max}=1-\frac{x_1}{2}[1-D(x_1,\eta)],\tag{7.10}$$

$$x_2^{min}=1-\frac{x_1}{2}[1+D(x_1,\eta)],\tag{7.11}$$

$$D(x_1,\eta)=\sqrt{\left(1-\frac{4\eta}{x_1^2}\right)\left(1-\frac{4\eta}{1-x_1+\eta}\right)}.\tag{7.12}$$

The allowed regions of the Dalitz plots for $J/\psi\to\gamma gg$ decays (open contour) and $J/\psi\to ggg$ (cross-hatched contour) for $m_g=0.721$ GeV are shown in Fig. 8(a). Similar contours for the corresponding Υ decays and $m_g=1.18$ GeV are shown in Fig. 8(b). The phase-space suppression factors due to gluon mass effects are the ratios of the areas inside the contours to the area above the dotted line, corresponding to $m_g=0$. It is seen that the phase-space suppression is considerable for Υ and very large for J/ψ decays.

The effect of the inclusion of longitudinal polarization states for the gluons is illustrated in Figs. 9 and 10, which show decay rates as a function of photon and gluon energies as given by Eq. (4.1) ($J/\psi\to\gamma gg$) and Eq. (7.6) ($J/\psi\to ggg$), respectively, for $m_g=0.721$ GeV. In Figs. 9(a) and 10(a) the longitudinal gluon contributions are suppressed by setting $\eta=0$ except in the equations defining the Dalitz plot boundary, i.e., only the phase-space limitations due to the nonvanishing value of m_g are taken into account. In Figs. 9(b) and 10(b) the complete formulas (4.1) and (7.6), respectively, are used. The most dramatic effect of the longitudinal contributions is a strong suppression of the decay rate for $J/\psi\to\gamma gg$ in the region $z\simeq 0.0$, $x_2\simeq 0.0$. As the experimental data analyzed here have $z\geqslant 0.3$, this has no practical consequences for the present work. Indeed, in the region of small z, the dominant mechanism of direct photon production is expected to be the fragmentation of light hadrons into photons [38,48], which is not taken into account in the NLO QCD calculation of Ref. [14]. As can be seen in Figs. 9(b) and 10(b) the other effect of the longitudinal contributions is a modest suppression of the decay rate, near the center of the allowed region of the Dalitz plot, relative to the boundaries. The gluon mass correction factors given by integrating Eq. (7.5) over z or Eq. (7.6) over x_1 and x_2, are presented in Table XI. The rows labeled ''LW'' use the complete formulas, and those labeled ''Phase space'' have $\eta=0$ except in the equations defining the kinematic limits. It can be seen that longitudinal gluon effects are negligible in the correction factors for $V\to ggg$ decays for both the J/ψ and the Υ. For $V\to\gamma gg$ decays these effects increase $f_{\gamma gg}$ by 30% and 8%, respectively, for the J/ψ and the Υ. The errors quoted on the correction factors are derived from the total errors on m_g given in Secs. V and VI above.

The values of $\alpha_s(m_c)$ and $\alpha_s(m_b)$ derived from Eqs. (7.2) and (7.3), taking into account gluon mass effects according to the values of $f_{ggg}/f_{\gamma gg}$ given in Table XI, are presented in Table XII (phase space corrections only) and Table XIII (full

TABLE XI. Gluon mass correction factors. ''Phase space'' indicates that gluon mass effects are taken into account only in the kinematic limits. ''LW'' means that the complete calculation of Ref. [39] is used. The errors quoted are derived from the total uncertainties in the fitted values of m_g. Note that $f_{\gamma gg}=f_{ggg}=1$ for $m_g=0$.

		$f_{\gamma gg}$	f_{ggg}	$f_{ggg}/f_{\gamma gg}$
J/ψ	Phase space	$0.40^{+0.07}_{-0.02}$	$0.18^{+0.08}_{-0.02}$	$0.45^{+0.10}_{-0.02}$
	LW	$0.52^{+0.06}_{-0.01}$	$0.18^{+0.07}_{-0.01}$	$0.35^{+0.09}_{-0.02}$
Υ	Phase space	$0.74^{+0.11}_{-0.04}$	$0.61^{+0.15}_{-0.06}$	$0.83^{+0.08}_{-0.04}$
	LW	$0.80^{+0.08}_{-0.03}$	$0.61^{+0.16}_{-0.06}$	$0.77^{+0.11}_{-0.05}$

TABLE XII. $\alpha_s(m_Q)$ values obtained including phase-space gluon mass corrections for different choices of the renormalization scale μ. See Table X for the definitions of Δ(PDG) and "Deviation." The quoted errors include the effect of the uncertainties in the gluon mass correction factors.

μ/m_Q	0.6	1.0	2.0	No $O(\alpha_s)$ correction
$\alpha_s(m_c)$	$0.221^{+0.002}_{-0.008}$	$0.298^{+0.016}_{-0.041}$	$0.467^{+0.062}_{-0.119}$	$0.525^{+0.066}_{-0.132}$
Δ(PDG)	-0.136 ± 0.027	-0.059 ± 0.025	0.110 ± 0.120	0.168 ± 0.133
Deviation (σ)	-5.0	-2.4	0.9	1.3
$\alpha_s(m_b)$	$0.189^{+0.005}_{-0.012}$	$0.193^{+0.008}_{-0.015}$	$0.221^{+0.035}_{-0.015}$	$0.248^{+0.015}_{-0.025}$
Δ(PDG)	-0.028 ± 0.009	-0.024 ± 0.011	0.004 ± 0.016	0.032 ± 0.025
Deviation (σ)	-3.1	-2.2	0.25	1.2

gluon mass corrections). In each case the values for $\mu/m_Q = 0.6$, 1.0 and 2.0 are presented as well as those given by neglecting the $O(\alpha_s)$ corrections in Eqs. (7.2) and (7.3). For all choices of renormalization scale, the agreement with the world average values is improved as compared to the values presented in Table X, where gluon mass effects are neglected. The best agreement [at the $(0.3–1.5)\sigma$ level] is found for $\mu/m_Q = 2.0$, though almost equally consistent results [deviations of $(1.2–1.7)\sigma$] are found when the $O(\alpha_s)$ corrections are neglected. The inclusion of longitudinal gluon effects, in the latter case, increases the value of $\alpha_s(m_c)$ by 30% and $\alpha_s(m_b)$ by 9%. These shifts are comparable to the uncertainties on α_s due to the experimental errors on R'_V and the gluon mass correction factors. Similar shifts are found for $\mu/m_Q = 2.0$ and somewhat smaller ones for $\mu/m_Q = 1.0$. The values of $\alpha_s(m_c)$ and $\alpha_s(m_b)$ given by using the full gluon mass correction with $\mu/m_Q = 1.0$ are compared, in Fig. 7, with the world average value of $\alpha_s(\mu)$, and the values obtained for the same renormalization scale, but without gluon mass corrections.

Comparison of Tables XII and XIII with Table X and inspection of Fig. 7 show that the inclusion of effective gluon mass corrections is essential in order to obtain values of $\alpha_s(m_c)$ and $\alpha_s(m_b)$, derived from measurements of R'_V, that are consistent with the current world average determination of $\alpha_s(Q)$.

Each of the published experiments extracted a value of α_s from the measured values of R'_Υ. In all cases, good consistency was found with other available measurements of α_s. This is due to the relatively large errors, at the time, both on the individual measurements and on the average value of the other measurements with which they were compared. It does not at all contradict the results shown in Table X, which show instead a poor consistency of values derived from the weighted average value of R'_Υ of the three latest experiments with the current world average value of α_s. The experiments CUSB, ARGUS, Crystal Ball, and CLEO all used the Brodsky-Lepage-Mackenzie (BLM) scale setting procedure [49] to determine α_s at a scale of $0.157M_\Upsilon$, i.e., 1.5 GeV. These results, together with their weighted mean, are presented in Table XIV. The mean value of $\alpha_s(1.5\ \text{GeV})$ of 0.228 ± 0.019 differs from the current world average value of $0.357+0.013-0.019$ by 4.8 standard deviations, and is consistent with the results for $\alpha_s(m_b)$ given in Table X. The CLEO2 experiment used the principle of minimal sensitivity (PMS) [50] to determine

$$\alpha_s(M_\Upsilon) = 0.163\pm0.002\pm0.009\pm0.010$$

where the first error is statistical, the second systematic, and the third due to the estimated uncertainty of the PMS scale setting procedure. Evolving to the scale $m_b = 4.9$ GeV using Eq. (7.4) gives

$$\alpha_s(m_b) = 0.190^{+0.020}_{-0.019}.$$

This differs from the current world average value cited above by only 1.3σ, but also agrees within $(0.19–1.1)\sigma$ with the values quoted in Table X. The latter, however, differ from the

TABLE XIII. $\alpha_s(m_Q)$ values obtained, including full gluon mass corrections from Ref. [39], for different choices of the renormalization scale μ. See Table X for the definitions of Δ(PDG) and "Deviation." The quoted errors include the effect of the uncertainties in the gluon mass correction factors.

μ/m_Q	0.6	1.0	2.0	No $O(\alpha_s)$ correction
$\alpha_s(m_c)$	$0.224^{+0.001}_{-0.005}$	$0.332^{+0.014}_{-0.042}$	$0.617^{+0.088}_{-0.178}$	$0.681^{+0.086}_{-0.187}$
Δ(PDG)	-0.133 ± 0.019	-0.025 ± 0.024	0.260 ± 0.178	0.324 ± 0.187
Deviation (σ)	-7.0	-1.0	1.5	1.7
$\alpha_s(m_b)$	$0.197^{+0.005}_{-0.016}$	$0.205^{+0.010}_{-0.022}$	$0.239^{+0.017}_{-0.033}$	$0.271^{+0.021}_{-0.040}$
Δ(PDG)	-0.020 ± 0.009	-0.012 ± 0.012	0.022 ± 0.033	0.054 ± 0.040
Deviation (σ)	-2.2	-1.0	0.67	1.4

TABLE XIV. Published values of α_s at the BLM scale determined from Υ radiative decays. For CLEO, the measured spectrum is extrapolated using the Field prediction. The first error quoted in each case is statistical, the second systematic.

Experiment	$\alpha_s(\mu_{BLM})=\alpha_s(1.5\ \text{GeV})$
CUSB	$0.226^{+0.067}_{-0.042}$
ARGUS	$0.225\pm0.011\pm0.019$
Crystal Ball	$0.25\pm0.02\pm0.04$
CLEO	$0.27^{+0.03\ +0.03}_{-0.02\ -0.02}$
Weighted mean	$0.228\pm0.016\pm0.011$

world average by $(3.0–6.0)\sigma$. The results of the present analysis and the combined average of those already published in the literature are thus in agreement, and lie 3σ or more below the world average. No consistent description is obtained unless the effective gluon mass effects are taken into account.

VIII. DISCUSSION

The inclusive photon spectrum for J/ψ decays (dashed curve) and Υ decays (solid curve) obtained from the fits performed here to all available experimental data are shown in Fig. 11. In both cases, the relativistic corrections and the Photiadis HO QCD correction are included. The values 0.721 GeV and 1.18 GeV of m_g found in Secs. V and VI above, are used for the J/ψ and Υ, respectively. It is clearly seen that the end-point suppression is much more severe for the J/ψ than the Υ. Also shown in Fig. 11 is the Field spectrum, which has been found to describe well all the measurements of the photon spectrum in $\Upsilon\rightarrow\gamma X$ except that of CUSB. It is seen to be in good qualitative agreement with the Υ fit curve,

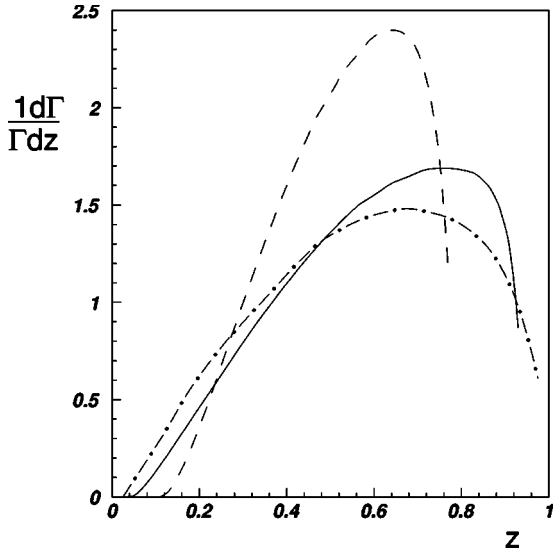

FIG. 11. Inclusive photon spectra including gluon mass effects. Dashed curve, $J/\psi\rightarrow\gamma X$, $m_g=0.721$ GeV, solid curve: $\Upsilon\rightarrow\gamma X$, $m_g=1.18$ GeV. The dot-dashed curve shows the Field [34] prediction for $\Upsilon\rightarrow\gamma X$.

but to predict a much harder spectrum than the fit curve for the J/ψ. In fact, the Field model, where the gluon mass is perturbatively generated using a low cutoff value of 0.45 GeV, predicts that the spectra are very similar in shape for the J/ψ and the Υ. This is clearly not the case.

The very different shapes of the spectra for the J/ψ and the Υ can only be understood if the scale introduced into the kinematics of the process by the effective gluon mass is not small in comparison with the mass of the J/ψ. This condition is very well satisfied, since the rest mass of the two effective gluons of $2\times0.721=1.44$ GeV is 47% of the J/ψ mass. As previously discussed in CF1 and CF2, the stronger suppression of the end point in J/ψ decays can be understood as a propagator effect acting on off-shell gluons if the genuine gluon mass is $\simeq1.0–1.5$ GeV, i.e., larger than the fitted value of m_g for the J/ψ, and similar to that found for the Υ. Corroborative evidence for this picture is provided by the structure of the hadronic final state. The dominance, for massive gluons, of the process $gg\rightarrow q\bar{q}$ over gluon splitting $gg\rightarrow ggg,ggq\bar{q},q\bar{q}q\bar{q}$ leads to a similar hadronic final state X in radiative J/ψ decays to that in the annihilation process $e^+e^-\rightarrow q\bar{q}$ at the same energy [13,16], consistent with the experimental observations.

The huge difference observed in the shape of the J/ψ and Υ spectra in Fig. 11 is clearly at variance with the principle of local parton hadron duality (LPHD) where parton level PQCD calculations are used (as in the Field model) down to scales of a few hundred MeV [52]. Indeed, in Monte Carlo models that give a good detailed description of hadronization effects [53,54] the cutoff scale of perturbative QCD effects is in the range 1–2 GeV, comparable to the effective gluon mass in Υ decays, and much larger than Λ_{QCD}. This point will be further discussed below.

Some remarks are now made on the related work presented in CF1 and CF2. In this case fits were performed only to the Mark II data for the J/ψ, and to those of ARGUS and Crystal Ball for the Υ. In the fit to the J/ψ, only phase-space gluon mass corrections were included, with no HO QCD or relativistic corrections. The Υ fits used phase-space gluon mass corrections and the Photiadis HO QCD correction, but no relativistic correction. The values obtained for m_g of 0.66 ± 0.01 GeV,[7] and 1.17 ± 0.08 GeV, respectively, are similar to those $0.721+0.016-0.068$ GeV, $1.18+0.09-0.29$ GeV, found in the present paper. The larger errors quoted here result from a study of theoretical systematics (relativistic corrections, different HO QCD corrections) not done in CF1 and CF2. Because of a programming error, the resolution functions used in these papers had a width that was too large by a factor $\sqrt{2}$. This had the effect of destroying the sensitivity of the high z part of the J/ψ spectrum to the process $J/\psi\rightarrow\gamma\eta'$. A fit with an acceptable confidence level was then obtained without explictly taking into account this decay channel as described in Sec. V above. An important difference between the present work and CF2 is an im-

[7]There is a misprint in CF1, propagated also to CF2, where this error is wrongly quoted as 0.08.

TABLE XV. Estimates of the value of the gluon mass from the literature. For Donnachie and Landshoff, the inverse of the correlation length a is quoted.

Author	Reference	Estimation method	Gluon mass
Parisi and Petronzio	[12]	$J/\psi \to \gamma X$	800 MeV
Cornwall	[8]	Various	500 ± 200 MeV
Donnachie and Landshoff	[59]	Pomeron parameters	687–985 MeV
Hancock and Ross	[61]	Pomeron slope	800 MeV
Nikolaev *et al.*	[62]	Pomeron parameters	750 MeV
Spiridonov and Chetyrkin	[63]	$\Pi^{\text{e.m.}}_{\mu\nu}$, $\langle \text{Tr}\, G^2_{\mu\nu} \rangle$	750 MeV
Lavelle	[64]	$qq \to qq$, $\langle \text{Tr}\, G^2_{\mu\nu} \rangle$	640 $\text{MeV}^2/Q(\text{MeV})$
Kogan and Kovner	[67]	QCD vacuum energy, $\langle \text{Tr}\, G^2_{\mu\nu} \rangle$	1.46 GeV
Field	[68]	PQCD at low scales (various)	$1.5^{+1.2}_{-0.6}$ GeV
Liu and Wetzel	[39]	$\Pi^{\text{e.m.}}_{\mu\nu}$, $\langle \text{Tr}\, G^2_{\mu\nu} \rangle$	570 MeV
		Glueball current, $\langle \text{Tr}\, G^2_{\mu\nu} \rangle$	470 MeV
Ynduráin	[66]	QCD potential	10^{-10}-20 MeV
Leinweber *et al.*	[69]	Lattice gauge	1.02 ± 0.10 GeV
Field	This paper	$J/\psi \to \gamma X$	$0.721^{+0.016}_{-0.068}$ GeV
		$\Upsilon \to \gamma X$	$1.18^{+0.09}_{-0.29}$ GeV

proved understanding of the effect of relativistic corrections. As is clear from the discussion at the beginning of Sec. II above, the ''binding energy'' $E(p)-m_{\text{Q}}$ introduced by KM must be a positive definite quantity. The same conclusion can be reached from simple physical reasoning. In the presence of the relativistic correction the heavy quark-antiquark annihilation process occurs over a finite spatial region around the origin of the radial wave function, instead of at the origin as in the static limit. As the ground state wave function peaks at the origin, relativistic corrections must always reduce the decay rate, not increase it. In CF2, following the NRQCD [18] approach, the corresponding parameter r was taken to be free, to be determined from experiment, and was allowed to take positive or negative values. In the present paper the relativistic correction parameter $\langle v^2 \rangle$ is set to the fixed values 0.28 and 0.09, respectively, for the J/ψ and Υ on the basis of potential model calculations. Finally, the NLO QCD correction to the inclusive photon spectrum [14] was not available when CF2 was written.

The analysis presented in this paper has neglected possible color octet contributions to the radiative decay rates. These have been calculated for Υ decays at NLO in the NRQCD formalism by Maltoni and Petrelli [55]. In the region of interest for the fits performed in the present paper, $z>0.3$, the corrections to the LO spectrum were found to be modest, $\simeq 10$–$15\,\%$. In a more recent study [56] in which octet operators were resummed to yield the so-called shape functions [57] a much larger contribution was predicted in the near end-point region. However, comparison with the CLEO2 data showed that the color octet contribution, with normalization fixed by the velocity counting rules of NRQCD, exceeds the experimental data by between one and two orders of magnitude. It may also be remarked that the result of the shape function calculation, in which clusters of ''nonperturbative'' soft gluons are summed, is expected to be drastically affected (reduced) if the phase-space suppression associated with a gluon mass of $\simeq 1$ GeV is taken into account. In view of the small correction to the shape of the spectrum due even to the full color singlet NLO correction [14] as compared to that resulting from gluon mass effects (see Figs. 3–6), the neglect of possible color octet contributions is not expected to modify, in any essential way, the conclusions of this paper. In fact, according to Ref. [56] the color octet contributions are expected to strongly enhance the rate in the end-point region, whereas what is observed is actually a strong suppression. Indeed, both color octet and color singlet NLO QCD corrections should be redone, taking into account gluon mass effects. Phase-space restrictions are expected, in this case, to significantly reduce the NLO corrections to both color singlet and color octet contributions, especially for J/ψ decays.

The values of the effective gluon mass determined, in the present paper, from radiative J/ψ and Υ decays are now compared with the results of other studies in the literature of gluon mass effects. A number of representative estimates of the gluon mass are presented in Table XV. In the following the generic symbol M_{g} will be used for the genuine gluon mass, reserving the symbol m_{g} for the ''effective mass'' in the sense described in Sec. IV above, determined at tree level in the radiative decays of heavy quarkonia to light hadrons.

Pioneering work in this field was done by PP [12]. An estimate of $\simeq 800$ MeV for the gluon mass was made from the observed softening of the end point of the inclusive photon spectrum in radiative J/ψ decays. The work presented in this paper is, in essence, a more refined version of the analysis of PP, taking into account experimental resolution effects, and including Υ decays as well as the best current knowledge on relativistic and HO QCD corrections.

The first extended theoretical discussion of gluon mass effects within QCD was made by Cornwall [8]. Estimates were made of the possible value of a dynamically generated

gluon mass by several different methods: phenomenological glueball regularization, considerations based on the gluon condensate, the glueball spectrum, and lattice gauge calculations. In fact, many of the gluon mass estimates shown in Table XV are based on the use of the gluon condensate

$$\langle \mathrm{Tr}\, G_{\mu\nu}^2 \rangle = \langle 0 | \alpha_s T[G_{\mu\nu}(x) G^{\mu\nu}(0)] | 0 \rangle = M_c^4 f\left(\frac{x^2}{a^2}\right) \tag{8.1}$$

introduced by Shiftman, Vainstein, and Zakharov (SVZ) [58]. Here $G_{\mu\nu}$ is the gluon field tensor. The gluon mass is related to the inverse of the correlation length a of the gluonic vacuum fields. In Ref. [58] the phenomenological determination of $\langle \mathrm{Tr}\, G_{\mu\nu}^2 \rangle$ by the use of QCD sum rules is described.

Donnachie and Landshoff [59] identified the Pomeron trajectory used to describe diffractive scattering with the QCD two-gluon exchange process [60]. They modified the perturbative gluon propagator in the long distance region by introducing a finite correlation length. The value of the latter was derived from phenomenological Pomeron exchange parameters. In Table XV the reciprocal of the correlation length is equated to the gluon mass. Other studies of the sensitivity of the Pomeron parameters to nonperturbative modifications of the gluon propagator were made by Hancock and Ross [61] and Nikolaev *et al.* [62]. Again, an effective gluon mass of about 800 MeV was found.

Spiridonov and Chetyrkin [63] estimated the gluon mass by calculating power corrections to the polarization tensor $\Pi_{\mu\nu}^{\mathrm{e.m.}}(q)$ of the electromagnetic current of light quarks, and identifying them with the gluon condensate term in the operator product expansion (OPE) for this quantity derived by SVZ. The calculation was later repeated by Liu and Wetzel [39], who obtained a very similar, though not identical, result (see below).

Lavelle [64], by considering a long-distance modification of the gluon propagator in the amplitude for quark-quark scattering, established a relation between a running, dynamically generated, gluon mass and the gluon condensate of SVZ. It was emphasized by Lavelle that the derived formula based on the OPE is valid only in the deep Euclidean region. Even so, in a recent paper Mihara and Natale (MN) [65] applied the running gluon mass formula of Lavelle to decays of the J/ψ and Υ to ggg of γgg where the gluons are either on shell or have timelike virtualities. MN concluded that the average effective gluon mass should be smaller for Υ than for J/ψ decays, at variance with the results of the fits presented in the present paper. The correction factors due to gluon mass effects f_{ggg} were calculated for the J/ψ and Υ and found to be 0.47 ± 0.30 and 0.94 ± 0.03, respectively, to be compared with the values found here (see Table XI) of $0.18 + 0.08 - 0.02$ and $0.61 + 0.16 - 0.06$. The smaller gluon mass corrections found by MN are unable to explain the large differences in the values of $\alpha_s(m_{\mathrm{Q}})$ determined from R_V' and the world average value of α_s (see Table X and Fig. 7).

The gluon mass estimates presented in Table XV are, with one exception, in the range from a few hundred MeV to about 1.5 GeV. The exception is the paper of Ynduráin [66] which claims that experimental upper bounds in the range from 20 MeV to 10^{-10} MeV may be set. These limits are based on considerations of the quantum mechanical potential between a quark and an antiquark. This is assumed to be Coulombic for short distances r $[r \ll (\Lambda_{QCD})^{-1}]$ where Λ_{QCD} is the QCD scale parameter, linear $[\simeq Kr, K \simeq (0.5)\ \mathrm{GeV}^2]$ for $(\Lambda_{QCD})^{-1} < r < m_{\mathrm{g}}^{-1}$, and, finally, for $r > m_{\mathrm{g}}^{-1}$, to exhibit a Yukawa form $\simeq e^{rm_{\mathrm{g}}}/r$. The linear portion of the potential gives rise to a barrier of height $E_{crit} \simeq K m_{\mathrm{g}}^{-1}$. Ynduráin argues that E_{crit} may be identified with the highest energy at which unsuccessful searches for liberated quarks have been performed. For example, $E_{crit} \simeq 200$ GeV leads to the limit

$$m_{\mathrm{g}} \simeq \frac{K}{200\ \mathrm{GeV}} = 2.5\ \mathrm{MeV}.$$

Other limits are given by applying similar arguments to the absence of proton decay into free quarks ($m_{\mathrm{g}} < 20$ MeV), and the nonobservation of free quarks on cosmological scales ($m_{\mathrm{g}} < 2 \times 10^{-10}$ MeV). The arguments leading to these limits are clearly untenable because of the neglect of the quantum field theory (QFT) aspects of the problem.[8] In fact, when a color field is stretched between a quark and an antiquark, the number of color charges is not conserved. The vacuum energy materializes as quark-antiquark pairs, which form bound states of light mesons (π, ρ, etc.). This mechanism, as implemented in the JETSET Monte Carlo program [53], is found to give a good description of the observed hadron multiplicity in $e^+e^- \to q\bar{q} \to$ hadrons, where the final state is just a color singlet $q\bar{q}$ pair of the type discussed by Ynduráin. This neglect of the QFT aspects of the problem renders it unecessary to discuss further the contradiction between Ynduráin's upper limits and the other gluon mass estimates in Table XV. It is interesting to note, however, that the paper of Ynduráin is the only one cited on the subject of experimental limits on the gluon mass in the current "Review of Particle Properties" [3].

The estimations of the gluon mass based on the phenomenologically determined value of the gluon condensate [58] cited in Table XV are, with one exception, in the range from 500 to 700 MeV. As discussed above, such a value for the gluon mass could not explain the much stronger suppression of the end point of the inclusive photon spectrum in J/ψ decays, as compared to Υ decays. The exception, which is much more consistent with the gluon mass value suggested

[8] Interestingly enough, Ynduráin mentions, near the end of his paper, the screening of the potential by quark pair production, but does not draw the conclusion that the existence of such effects invalidate his limits on m_{g} derived from a pure quantum mechanical potential. In the real world it is impossible to deconfine a quark since the production of low mass $q\bar{q}$ pairs (mesons) is always energetically favored.

by the radiative decays, is the calculation of Kogan and Kovner [67]. This uses an analytical approach in which the vacuum energy of a gauge-invariant QCD wave functional is minimized. It leads to the relation, for a pure SU(3) Yang-Mills theory,[9]

$$\langle \mathrm{Tr}\, G_{\mu\nu}^2 \rangle = \frac{1}{40\pi} M_g^4 . \tag{8.2}$$

Substituting the value of $\langle \mathrm{Tr}\, G_{\mu\nu}^2 \rangle$ of 0.038 GeV^4 from Ref. [58] gives $M_g = 1.48$ GeV. This value is quite consistent with the effective gluon masses derived earlier [15,16] and confirmed in the present study. It also agrees well with a previous, independent, estimate of the present author, based on a PQCD analysis of several processes with low physical scales [68], and a recent lattice gauge estimate [69].

An effective gluon mass has also been introduced in the context of the estimation of power- corrections to various hard QCD processes [70]. This was already briefly discussed in CF2. The leading correction to the mean thrust in e^+e^- annihilation into hadrons, for example, is found to be $\simeq M_g/\sqrt{s}$. The gluon mass appears as an intermediate parameter in these calculations, but no explicit values are quoted, and to date no comparisons have been made with other estimates of the effective gluon mass, e.g., lattice calculations. Power corrections are an example of ''higher twist'' effects in the language of the OPE formalism. In fact, it was pointed out in Ref. [58] that, as a consequence of the dimensionality of the relevant operators, physical systems described by an OPE (as in the case of QCD sum rules) are expected to have a leading power correction $\simeq 1/Q^4$. An OPE description, as used in QCD sum rules, is not appropriate to describe higher twist effects in the quarkonium radiative decay spectrum discussed in the present paper. As can be seen by inspection of Eqs. (7.5) and (7.6) the leading higher twist effects are $\simeq (m_g/Q)^2$ where $Q = M_V$.

The gluon mass estimate labeled ''PQCD at low scales'' in Table XV, is based on phenomenological arguments (similar to those used later in Ref. [67]), proposed in Ref. [71] and further developed in Refs. [68,72,73]. In this approach, effective gluon and quark masses are related to the QCD Λ parameter, which plays the role of an infrared cutoff of the theory.

It is interesting to note that the approach just mentioned, which relates the Λ parameter of PQCD to effective quark and gluon masses, is complementary to the SVZ approach of describing the perturbative/nonperturbative interface in terms of QCD sum rules. In this context it is interesting to consider the relation between α_s, $\langle \mathrm{Tr}\, G_{\mu\nu}^2 \rangle$, and M_g [63]:

$$\langle \mathrm{Tr}\, G_{\mu\nu}^2 \rangle = \frac{\alpha_s(Q^2)}{\pi^2} M_g^4 \left(3 \ln \frac{Q^2}{M_g^2} + \frac{23}{2} - 12\zeta(3) \right). \tag{8.3}$$

The value $M_g = 750$ MeV quoted in Table XV was obtained by setting $Q = 10$ GeV in Eq. (8.3), but the equation is expected to be valid for any value of Q in the perturbative region. Substituting the values $Q_0 = 2.88$ GeV, $\alpha_s(Q_0^2) = \alpha_s(0) = 0.27$, and $M_g = 1.0$ GeV, which reproduce well the measured value of $\alpha_s(M_Z^2)$ [68], into Eq. (8.3) gives, for the gluon condensate, $\langle \mathrm{Tr}\, G_{\mu\nu}^2 \rangle = 0.094$ (GeV)^4, which may be compared with the average value derived by Narison [75] of $\langle \mathrm{Tr}\, G_{\mu\nu}^2 \rangle = 0.071 \pm 0.009$ (GeV)^4. Liu and Wetzel [39] derived a formula identical to Eq. (8.3) except that the term 23/2 is replaced by 10. With the same parameters as quoted above, the value $\langle \mathrm{Tr}\, G_{\mu\nu}^2 \rangle = 0.053$ (GeV)^4 is obtained. In view of the factor of $\simeq 2$ difference between the original SVZ estimation of the numerical value of $\langle \mathrm{Tr}\, G_{\mu\nu}^2 \rangle$, as compared to that of Narison, the overall consistency of the value of $\langle \mathrm{Tr}\, G_{\mu\nu}^2 \rangle$ derived from the QCD sum rule approach and from the PQCD phenomenology of Ref. [68], is very satisfactory.

Thus, although gluon mass effects are only *directly* observable in processes with pure gluonic parton-level final states, such as the radiative heavy quarkonia decays analyzed in detail in this paper, the existence of a gluon mass of order 1 GeV is already implicit in all PQCD analyses that use, as an infrared cutoff, the conventional Λ parameter. It is important to stress, however, that, as previously pointed out [73,74], the scale at which PQCD is expected to break down is $\simeq$ gluon mass $\simeq 1$ GeV, *not* Λ_{QCD}, which is typically a factor of 5 smaller. It is interesting to note that the same conclusion has recently been reached in a study of the five-loop QCD β function, using Padé approximant methods [51]. From this point of view the success of PQCD, in association with the LPHD hypothesis, in describing observed particle multiplicity distributions, as well as their energy dependence, using cutoff scales Q_0 as low as 270 or even 150 MeV [52], seems somewhat mysterious and may be accidental. As previously mentioned, Monte Carlo generators that actually simulate in detail both the partonic and hadronic phases of the space-time evolution of the final state use infrared cutoff parameters of about 1–2 GeV, of the same order as the observed gluon mass.

Since the main effect of the inclusion of a phenomenological gluon mass on the QCD predictions is phase-space suppression, it is clear that the associated mass must be timelike: $m_g^2 > 0$. This behavior is also consistent with an analytical parametrization of the lattice results of Ref. [69]. Another recent lattice study using a Coulomb gauge gluon propagator [76] has suggested rather a *pure imaginary* pole mass: $i(575 \pm 124)$ MeV. This work is related to the suggestion of Gribov [77] that color confinement is due to a long range Coulomb force. In this model physical (transverse) gluons disappear from the physical spectrum in the infrared region. This would appear to be at variance with the essential role of massive, timelike, and dominantly transverse physical gluons in the description of inclusive photon spectra that is demonstrated in the present paper. Actually, renormalizability remains to be proved for the Coulomb gauge and, as pointed out by the authors of Ref. [76], except possibly in a confined phase, in quantum field theory the square of a particle mass

[9]That is, effects of quark fields are neglected.

identified with the pole of a propagator must be real and positive. The author's opinion is that pure quantum field theory studies of the type carried out by Gribov and Zwanziger [78] are no better adapted than the quantum mechanical potential model of Yndurain [66], discussed above, to understand the physical mechanism of confinement. This appears to occur via a transition beween partonic and hadronic phases of matter, after which color charges are all confined within hadrons, which are mostly bound states of quarks. Clearly quenched lattice calulations of the type done in Ref. [76] are unable to describe such a mechanism.

It has recently been pointed out that the introduction of a term containing a tachyonic gluon mass λ with $\lambda^2 \simeq -0.5\ \mathrm{GeV}^2$ in the OPE of QCD sum rules is able to explain some long standing puzzles in the related phenomenology [79]. This approach was justified by evidence from lattice gauge calculations for nonperturbative contributions leading to a linearly increasing term in the static QCD potential at short distances [80]. The connection of this gluon mass parameter, which gives an economical description, within the QCD sum rule formalism, of a nonperturbative *short distance* effect, with the timelike effective mass discussed in the present paper (and all references cited in Table XV) is unclear. This latter mass describes rather the *long distance* behavior of the gluon propagator. It is quite possible that both the timelike and tachyonic gluon masses may be appropriate and consistent phenomenological parameters within their different domains of applicablity.

IX. SUMMARY AND OUTLOOK

In this paper a phenomenological QCD analysis has been performed using all available data on the inclusive photon spectrum in the decays of the J/ψ (Mark II Collaboration) and the Υ (CUSB, ARGUS, Crystal Ball, and CLEO2 Collaborations). The fits performed to the shape of the spectra included, for the first time, the combined contributions of relativistic corrections, NLO PQCD corrections, and corrections due to the nonvanishing gluon mass. For the relativistic correction, fixed values of $\langle v^2 \rangle$ of 0.28 and 0.09 were assumed for the J/ψ and Υ, respectively, in accordance with recent potential model calculations. Both the new, complete, NLO PQCD calculation by Krämer [14] of the Υ photon spectrum and the old resummed calculation of Photiadis [17] (applicable only in the end-point region $z \simeq 1$) were used in the fits. Gluon mass effects were estimated using the complete tree level calculation of $V \rightarrow \gamma gg$ of Liu and Wetzel [39].

For neither the J/ψ nor the Υ was any consistent description of the experimental data possible in the absence of gluon mass corrections. In this case, for the Mark II data, no fit was obtained with a confidence level greater than 10^{-30} (Table V). For the Υ, acceptable confidence levels of 0.17 and 0.13 were found for some fits to the Crystal Ball and CLEO2 data, but not for ARGUS where the best confidence level obtained was 6.7×10^{-3} (Table VII). However, the best confidence level for the combined fit to these three experiments was only 4.7×10^{-3}.

Including gluon mass corrections yielded confidence levels of greater than 1% for all the fit hypotheses tried (see Tables VI and VIII) and values of the effective gluon mass m_g of

$$m_g = 0.721^{+0.010\ +0.013}_{-0.009\ -0.068}\ \mathrm{GeV} \quad (J/\psi) \quad (\text{Mark II}),$$

$$m_g = 1.18^{+0.06\ +0.07}_{-0.06\ -0.28}\ \mathrm{GeV} \quad (\Upsilon)$$

(mean of ARGUS, Crystal Ball, and CLEO2).

The first errors quoted are experimental, and correspond to the 68% error contour of the fit, while the second errors are theoretical, reflecting the spread in the best fit values of m_g resulting from different treatments of relativistic and HO PQCD corrections. It is clear from the fit results shown in Tables VI and VIII that the shape of the photon spectrum for both the J/ψ and the Υ is completely dominated by gluon mass effects. Introducing the relativistic correction leaves the fitted values of m_g almost unchanged, while the shifts produced by different HO PQCD corrections are less than, or comparable to, the fit errors. The gluon mass corrections are due essentially to phase-space restrictions. Including or excluding contributions from longitudinal gluon polarization states changes the fitted values of m_g by only $\simeq 5\%$.

It can be seen, from the theoretical photon spectra calculated including the effects given by the experimentally determined values of m_g (Fig. 11) that the suppresssion of the end point of the spectrum is much stronger in the case of the J/ψ than that of the Υ. This is in contradiction with the prediction of the QCD parton shower model of Field [34], which agrees well with the measured Υ spectrum, but predicts, for the J/ψ, a much harder spectrum than that actually observed. Such a strong suppression of the J/ψ end point, in comparison with that of the Υ, is possible only if the gluon mass is $\simeq 1$ GeV. All these conclusions are in agreement with those of two earlier, closely related, papers [15,16], in which it was conjectured, following the work of Parisi and Petronzio [12], that gluon mass corrections must be much more important than either relativistic on HO PQCD corrections in determining the shapes of the inclusive photon spectra.

The QCD coupling constants $\alpha_s(1.5\ \mathrm{GeV})$ and $\alpha_s(4.9\ \mathrm{GeV})$ were determined from the experimental measurements of the branching ratio R'_V [Eq. (7.1)] for the J/ψ and Υ, respectively. Use of R'_V has the advantage of being insensitive to relativistic correction effects. As shown in Fig. 7, even allowing for a variation of the renormalization scale in the range from $0.6m_Q$ to $2.0m_Q$, poor agreement (deviations of $>4.8\sigma, 3.0\sigma$ for the $J/\psi, \Upsilon$, respectively) is found with the current world average value of $\alpha_s(Q)$. Using the measured m_g values to calculate the gluon mass correction factors in the theoretical expressions for R'_V [Eqs. (7.2) and (7.3)] leads to values of α_s that are consistent, albeit within much larger errors (due mainly to the large theoretical error on m_g), with the expected value of $\alpha_s(Q)$ (see Fig. 7).

The results obtained in this paper for the effective gluon mass in radiative J/ψ and Υ decays are compared, in Table XV, with some other estimates of the gluon mass that have

appeared in the literature over the last 20 years. Apart from the upper limits of Yndurain [66], which have been critically discussed in the previous section of this paper, all the estimates lie in the range from 500 MeV to 1.5 GeV. The values of m_g obtained here favor somewhat higher values of the genuine gluon masss M_g of $\geqslant 1$ GeV. In particular, there is good agreement with the estimates of Kogan and Kovner [67] (minimization of the energy of a pure Yang-Mills QCD wave functional), a previous estimate of the present author, using a PQCD analysis of several processes with low physical scales, and the recent lattice gauge estimate of Leinweber *et al.* [69] with improved lattice sampling in the far infrared region. It is also mentioned in the previous section that the conventional value for the phenomenological scale parameter Λ of PQCD of several hundred MeV actually implies a gluon mass some five times larger. Since for scales less than M_g Λ is actually a (calculable) scale dependent parameter [71], there is no Landau pole in QCD at the scale $Q=\Lambda$, but rather a breakdown of PQCD at a much larger infrared cutoff scale $Q_0 \geqslant 1$ GeV.

A model of confinement in which a purely imaginary gluon mass is introduced [76] predicts the decoupling of physical gluon states at low physical scales. Such behavior would seem to be inconsistent with the radiative decay data which can only be described by the contribution, in the same infrared region, of physical gluons with a timelike effective mass.

A contribution in the OPE of QCD sum rules corresponding to a tachyonic gluon mass was recently proposed [79] to describe some short distance properties of the QCD potential suggested by lattice studies [80]. This work has no obvious connection with the present one where it is shown instead that a gluon with a timelike effective mass apparently plays an important role in the long distance region.

Since the theoretical uncertainties on the values of the effective gluon mass m_g determined here are much larger than the experimental ones [the former are $9\%(J/\psi)$ and $23\%(\Upsilon)$ as compared to $1.3\%(J/\psi)$ and $5\%(\Upsilon)$ for the latter] the most urgent need is for improved theory predictions rather than more precise experimental data.[10] As a first step, NLO PQCD calculations should be repeated including gluon mass effects, as has been done at tree level by Parisi and Petronzio and Liu and Wetzel. Of even more interest may be the calculation of

$$J/\psi \rightarrow \gamma q \bar{q}$$

via the exchange of two massive virtual gluons (actually a NNLO process) to test the conjectured dominance of this process as already indicated by the structure of the hadronic final state.

As was already evident from previously presented results [16], the usefulness of the NRQCD approach of Ref. [18] will be very limited unless some means is found of incorporating the numerically very important gluon mass effects within the formalism. Another important problem that this approach must address is the possible double counting of PQCD and relativistic corrections [73].

Finally, it should not be forgotten that the most dramatic effects discussed in this paper (in the process $J/\psi \rightarrow \gamma X$) are based on the results of a single experiment [13] performed more than 20 years ago now. It is clearly important that this remarkable experimental result, strongly suggesting that the gluon mass is $\simeq 1$ GeV, should be confirmed. In a world where half dozen or so *b* factories (or their equivalents) exist, or are under construction, it is high time that the τ charm-quark energy region be revisited with modern general-purpose detectors and much higher integrated luminosity than that which yielded the data from the Mark II collaboration that have been analyzed in this paper.[11] In view of the less than perfect consistency of the different measurements of $\Upsilon \rightarrow \gamma X$, an improved measurement of this process, with at least an order of magnitude greater statistics, and reduced systematic errors, would be of great interest. This is perhaps possible at existing *b* factories.

ACKNOWLEDGMENTS

I especially thank M. Consoli for a collaboration that is at the inception of the work described in this paper. I thank S. Catani, M. Krämer, M. Mangano, and D. Ross for their interesting critical comments. Finally, I am indebted to D. Duchesneau for a careful reading of the manuscript, and a discussion that helped to improve the clarity of the presentation.

APPENDIX

In the previously published analysis of the J/ψ and Υ inclusive photon spectra [16], resolution effects were simulated by smearing the theoretical distributions with a Gaussian random number. In order to obtain stable fit results, an unsmeared histogram with a very large number of entries was necessary, and the random number throwing had to be repeated at each fit iteration, which both was time consuming and resulted in different statistical errors in the fitted function at each iteration. Even with $\simeq 10^6$ events in the histogram, the determination of the exact position of the χ^2 minimum was quite difficult. To avoid these problems, a new, purely analytical smearing technique was used for the fits presented in this paper. The method was faster and eliminated all problems related to the statistical errors inherent in Monte Carlo methods.

A theoretical histogram of the inclusive photon spectrum,

[10] It is interesting to note that the effective gluon mass is determined with a much better relative precision for the J/ψ than for the Υ. This is a consequence of the larger size of the gluon mass corrections for the J/ψ resulting in a greater sensitivity to m_g.

[11] It seems, at the time of writing, that there is now a very good chance that this will soon be done [82].

with bin index J, $H0(J)$, is generated with a fine binning, typically $NBIN=1000$. The corresponding resolution smeared histogram with bin index JS, $HS(JS)$, is generated according to the following algorithm:

$$HS(JS)=\sum_{J=1}^{NBIN} H0(J)F(J,JS)$$

where

$$F(J,JS)=\begin{cases}\dfrac{\exp\left[-\dfrac{1}{2}\Delta(J,JS)^2\right]}{\sigma[z(J)]}, & -6\leqslant\Delta(J,JS)\leqslant 6\\ 0.0, \quad \Delta(J,JS)>6, \quad \Delta(J,JS)<-6, & \end{cases} \tag{A1}$$

and

$$\Delta(J,JS)=\frac{z(J)-z(JS)}{\sigma[z(J)]}.$$

Here $z(J)$ is the central value of the scaled photon energy in bin J and $\sigma[z(J)]$ is the photon energy resolution at energy $E_\gamma=z(J)M_V/2$. Values of $\sigma[E_\gamma]/E_\gamma$ for the different experiments analyzed here are reported in Table II. In this way, a Gaussian resolution smearing of the photon energy by up to $\pm 6\sigma$ around the true value is performed. Precise results were obtained by normalizing the unsmeared histogram to a million events:

$$\sum_{J=1}^{NBIN} H0(J)=10^6,$$

but, unlike in the case of a Monte Carlo simulation, the execution time of the program does not depend on this number. The bins of the smeared histogram are grouped to correspond to those of the experimental histogram before fitting [81]. In all the fits the relative normalization of the experimental and the smeared theoretical histogram was allowed to float.

[1] H. Frizsch, M. Gell-Mann, and H. Leutwyler, Phys. Lett. **47B**, 365 (1973).
[2] S. Weinberg, Phys. Rev. Lett. **31**, 494 (1973).
[3] Particle Data Group, D.E. Groom *et al.*, Eur. Phys. J. C **15**, 1 (2000).
[4] C.H. Lewellyn Smith, Phys. Lett. **46B**, 233 (1973).
[5] J.M. Cornwall, D.N. Levin, and G. Tiktopoulos, Phys. Rev. Lett. **30**, 1268 (1973).
[6] J.C. Pati and A. Salam, Phys. Rev. D **8**, 1240 (1973); **10**, 275 (1974); R.N. Mohapatra, J.C. Pati, and A. Salam, *ibid.* **13**, 1733 (1976); A. de Rujula, R.C. Giles, and R.L. Jaffe, *ibid.* **17**, 285 (1978); **22**, 227 (1980); T. Goldman and G.L. Shaw, Phys. Rev. Lett. **47**, 887 (1981); E.W. Kolb, G. Steigman, and M.S. Turner, *ibid.* **47**, 1357 (1981); G. Rajasekaran and S.D. Rindani, Phys. Lett. **99B**, 361 (1981); Prog. Theor. Phys. **67**, 1505 (1982); A.Yu. Ignatiev *et al.*, Theor. Math. Phys. **47**, 373 (1981).
[7] J.M. Cornwall, Nucl. Phys. **B157**, 392 (1979).
[8] J.M. Cornwall, Phys. Rev. D **26**, 1453 (1982).
[9] G. Curci and R. Ferrari, Nuovo Cimento Soc. Ital. Fis., A **32A**, 151 (1976).
[10] G. Curci and E. d'Emilio, Phys. Lett. **83B**, 199 (1979).
[11] J.R. Forshaw, J. Papavassiliou, and C. Parrinello, Phys. Rev. D **59**, 074008 (1999).
[12] G. Parisi and R. Petronzio, Phys. Lett. **94B**, 51 (1980).
[13] Mark II Collaboration, D.L. Scharre *et al.*, Phys. Rev. D **23**, 43 (1981).
[14] M. Krämer, Phys. Rev. D **60**, 111503 (1999).
[15] M. Consoli and J.H. Field, Phys. Rev. D **49**, 1293 (1994).
[16] M. Consoli and J.H. Field, J. Phys. G **23**, 41 (1997).
[17] D.M. Photiadis, Phys. Lett. **164B**, 160 (1985).
[18] G.T. Bodwin, E. Braaten, and G.P. Lepage, Phys. Rev. D **51**, 1125 (1995).
[19] R. van Royen and V.F. Weisskopf, Nuovo Cimento A **50**, 617 (1967).
[20] H. Bergström, H. Snellman, and G. Tengstrand, Phys. Lett. **82B**, 419 (1979).
[21] W.Y. Keung and I.J. Muzinich, Phys. Rev. D **27**, 1518 (1983).
[22] H.A. Bethe and E.E. Salpeter, Phys. Rev. **82**, 309 (1951); **84**, 1232 (1951).
[23] G. A. Schuler, ''Quarkonium Production and Decays,'' Report No. CERN-TH.7170/94, 1994.
[24] See, for example, C.T.H. Davies *et al.*, Phys. Rev. D **50**, 6963 (1994); C.T.H. Davies *et al.*, *ibid.* **52**, 6519 (1995).
[25] H.C. Chiang, J. Hüfner, and H.J. Pirner, Phys. Lett. B **324**, 482 (1994).
[26] K-T. Chao, H.-W. Huang, and Y.-Q. Liu, Phys. Rev. D **53**, 221 (1996).
[27] G.A. Schuler, in *Proceedings of the UIC Quarkonium Physics Workshop*, Chicago, 1996, edited by H. Goldberg, T. Imbo, and W. Y. Keung [Int. J. Mod. Phys. A **12**, 3951 (1997)].
[28] M. Beyer *et al.*, Z. Phys. C **55**, 307 (1992).
[29] A. Bradley, Phys. Lett. **77B**, 422 (1978).
[30] E. Eichten *et al.*, Phys. Rev. D **21**, 203 (1980).
[31] H. Bergström, H. Snellman, and G. Tengstrand, Phys. Lett. **80B**, 242 (1979).
[32] H. Bergström, H. Snellman, and G. Tengstrand, Z. Phys. C **4**, 215 (1980).
[33] A. Ore and J.L. Powell, Phys. Rev. **75**, 1696 (1949).
[34] R.D. Field, Phys. Lett. **133B**, 4 (1983).
[35] Ya.I. Azimov *et al.*, Phys. Lett. **165B**, 147 (1985).
[36] B.I. Ermolayev and V.S. Fadin, JETP Lett. **33**, 269 (1981); A.H. Mueller, Phys. Lett. **104B**, 161 (1981).
[37] A.E. Chudakov, Izv. Akad. Nauk SSSR, Ser. Fiz. **19**, 650 (1955).
[38] F. Hautmann, in *Proceedings of PHOTON '97*, Egmond an

Zee, The Netherlands, 1997, edited by A. Buijs and F. C. Erné (World Scientific, Singapore, 1998), p. 68.
[39] J.-P. Liu and W. Wetzel, ''Gluon-Mass Effects in Quarkonia Decays, e^+e^- Annihilation and the Scalar Glueball Current,'' University of Heidelberg, Report No. HD-THEP-96-47, hep-ph/9611250.
[40] L. Köpke and N. Wermes, Phys. Rep. **174**, 67 (1989).
[41] R.D. Schamberger *et al.*, Phys. Lett. **138B**, 225 (1984).
[42] CLEO Collaboration, A. Bean *et al.*, Phys. Rev. Lett. **56**, 1222 (1986).
[43] ARGUS Collaboration, H. Albrecht *et al.*, Phys. Lett. B **199**, 291 (1987).
[44] Crystal Ball Collaboration, A. Bizzeti *et al.*, Phys. Lett. B **267**, 286 (1991).
[45] CLEO II Collaboration, B. Nemati *et al.*, Phys. Rev. D **55**, 5273 (1997). This publication did not present an acceptance corrected spectrum. The spectrum used here was taken from Contributed Paper 274 to the XVI International Symposium on Lepton and Photon Interactions, Ithaca, NY, 1993; F. Muheim (private communication).
[46] W. Kwong *et al.*, Phys. Rev. D **37**, 3210 (1988).
[47] Particle Data Group, C. Caso *et al.*, Eur. Phys. J. C **3**, 1 (1998).
[48] S. Catani and F. Hautmann, Nucl. Phys. B (Proc. Suppl.) **39BC**, 359 (1995).
[49] S.J. Brodsky, G.P. Lepage, and P.B. Mackenzie, Phys. Rev. D **28**, 228 (1983).
[50] P.M. Stevenson, Phys. Rev. D **23**, 2916 (1981); S. Sanghera, Int. J. Mod. Phys. A **9**, 5743 (1994).
[51] F.A. Chishtie, V. Elias, and T.G. Steele, Phys. Lett. B **514**, 279 (2001).
[52] See, for example, V.A. Khoze, S. Lupia, and W. Ochs, Eur. Phys. J. C **5**, 77 (1998).
[53] T. Sjöstrand, Comput. Phys. Commun. **82**, 74 (1994).
[54] G. Marchesini *et al.*, Comput. Phys. Commun. **67**, 465 (1992).
[55] F. Maltoni and A. Petrelli, Phys. Rev. D **59**, 074006 (1999).
[56] S. Wolf, Phys. Rev. D **63**, 074020 (2001).
[57] I.Z. Rothstein and M.B. Wise, Phys. Lett. B **402**, 346 (1997); M. Beneke, I.Z. Rothstein, and M.B. Wise, *ibid.* **408**, 373 (1997); M. Beneke, G.A. Schuler, and S. Wolf, Phys. Rev. D **62**, 034004 (2000).
[58] M.A. Shiftman, A.I. Vainstein, and V.I. Zakharov, Nucl. Phys. **B147**, 385 (1979); **B147**, 448 (1979).
[59] A. Donnachie and P.V. Landshoff, Nucl. Phys. **B311**, 509 (1989).
[60] F.E. Low, Phys. Rev. D **12**, 163 (1975); S. Nussinov, Phys. Rev. Lett. **34**, 1286 (1975); L.V. Gribov, E.M. Levin, and M.G. Ryskin, Phys. Rep. **100**, 1 (1983).
[61] R.E. Hancock and D.A. Ross, Nucl. Phys. **B394**, 200 (1993); see also J.R. Forshaw and D.A. Ross, *Quantum Chromodynamics and the Pomeron* (Cambridge University Press, Cambridge, England, 1997), p. 131.
[62] M.N. Nickolaev, B.G. Zakharov, and V.R. Zoller, Phys. Lett. B **328**, 486 (1994).
[63] V.P. Spiridonov and K.G. Chetrykin, Yad. Fiz. **47**, 818 (1988) [Sov. J. Nucl. Phys. **47**, 522 (1988)].
[64] M. Lavelle, Phys. Rev. D **44**, R26 (1991).
[65] A. Mihara and A.A. Natale, Phys. Lett. B **482**, 378 (2000).
[66] F.J. Yndurán, Phys. Lett. B **345**, 524 (1995).
[67] I.I. Kogan and A. Kovner, Phys. Rev. D **52**, 3719 (1995).
[68] J.H. Field, Int. J. Mod. Phys. A **9**, 3283 (1994).
[69] D.B. Leinweber *et al.*, Phys. Rev. D **60**, 094507 (1999).
[70] Yu.L. Dokshitzer and B.R. Webber, Phys. Lett. B **352**, 451 (1995); Yu.L. Dokshitzer, G. Marchesini, and B.R. Webber, Nucl. Phys. **B469**, 93 (1996).
[71] J.H. Field, Ann. Phys. (N.Y.) **226**, 209 (1993).
[72] J.H. Field, Mod. Phys. Lett. A **11**, 2921 (1996); **12**, 217(E) (1997).
[73] J.H. Field, Nucl. Phys. B (Proc. Suppl.) **54A**, 247 (1997).
[74] J.R. Cudell, A. Donnachie, and P.V. Landshoff, Nucl. Phys. **B322**, 51 (1989).
[75] S. Narison, Phys. Lett. B **387**, 162 (1996).
[76] A. Cucchieri and D. Zwanziger, Phys. Lett. B **524**, 123 (2002).
[77] V.N. Gribov, Nucl. Phys. **B39**, 1 (1978).
[78] D. Zwanziger, Nucl. Phys. **B518**, 237 (1998).
[79] K.G. Chetrykin, S. Narison, and V.I. Zakharov, Nucl. Phys. **B550**, 353 (1999).
[80] G.S. Bali, Phys. Lett. B **460**, 170 (1999).
[81] The function minimization and error analysis program MINUIT was used. See CERN Program Library Long Write-Up D506, March 1994.
[82] H. Stöck, ''The CLEO-c Project–A New Frontier of QCD Physics,'' talk presented at the XXXVIIth Recontres de Moriond: QCD and High Energy Hadronic Interactions, Les Arcs, France, hep-ex/02040125.